E-ISSN: 1116 - 2759 P-ISSN: 3027-0111
MPRI-EDIR
INTERNATIONAL JOURNAL OF EARTH DESIGN AND INNOVATION RESEARCH
VOL. 12 NO. 4 – APRIL, 2026

QUALITATIVE INTERPRETATION AND LITHO-STRUCTURAL EVALUATION STUDIES WITH DEPTH ESTIMATION ANALYSIS FOR HYDROCARBON AND SOLID/ORE MINERAL EXPLORATIONS USING HIGH-RESOLUTION AEROGRAVITY DATA IN PARTS OF SOKOTO BASIN, NORTHWESTERN NIGERIA

ISHOLA, S. A

Department of Earth Sciences, Faculty of Science, Olabisi Onabanjo University Ago-Iwoye, P.M.B 2002, Ago-Iwoye, Ogun State, Nigeria

Corresponding Author:
ishola.sakirudeen@oouagoiwoye.edu.ng

DOI: https://doi.org/10.70382/mejedir.v12i4.082

Abstract

The renewed quests for hydrocarbon prospecting and boosting the National and continental economies have intensified in the search for viable oil and gas reserves in Nigeria. These have reawakened the interests of stakeholders in energy/oil and gas matters in Sokoto basin as a potential zone for hydrocarbon potential. The study was undertaken for the purpose of unravelling and characterizing the litho-structural styles and regional trends of the earths sequence covering parts of Sokoto basin, Northwestern Nigeria with a view of delineating hydrocarbons and solid/ore mineral potentials in the area. Aerogravity datasets of parts of Sokoto Basin comprising of four (4) sheets (72,73, 95 and 96) were acquired from the Nigerian Geological Survey Agency (NGSA) by Bureau Gravimetrique Internationale (BGI), France. These datasets were acquired using a fixed-wing aircraft and processed to produce Bouguer anomaly map. Qualitative analysis was carried out using various Filtering techniques, including two-dimensional

Keywords:
Characterization, Delineation, Aerogravity, Qualitative Interpretation, Causative bodies, Analytical Signal

EDITOR-IN-CHIEF
Prof. W. F. HILL [MALAWI]

First Fourier transform (FFT2D), analytic signal, and horizontal and vertical derivatives. These enhanced data sets facilitated the mapping of structural features, faults, and potential reservoir seals. The Quantitative analysis was carried out using Euler Deconvolution technique to estimate depth and define subsurface structures. The gravity values in the total field ranged from -71.67 to -28.26 mgal. The Analytical signal revealed amplitude signal that varied from 0.00027 to 0.00107 mgal/m. numerical values of the derivatives ranged from -0.00141 to 0.00107mgal, -0.00098 to 0.00091 and -0.00091 to 0.00090 mgal/m respectively reported for first vertical and first horizontal (along X and Y-direction) derivatives. The 3D Euler Deconvolution techniques revealed the depth and locations of causative bodies that yielded the gravity field was found to be in the minimum range of 1482 to 2514m at an average depth of 2032m and the maximum range of 5653 to 6487m at an average depth of 6040m for structural Index zero (S.I = 0). Overall, the study revealed significant information on basin thickness, faulting, intrusive bodies, and structural configurations, providing essential data for resource exploration and development in the investigated area for local, national, and international benefits.

Introduction

Geophysical methods are the study of the physical properties of the earth, atmosphere, and space. It involves techniques used to explore and investigate the subsurface of the earth. The objectives of a geophysical survey are to locate subsurface geological structures or causative bodies, where it is possible to measure their dimension or relevant physical properties as well as locating potential mineral and hydrocarbon deposit, and estimating their size and quality. a

The aim of gravity method is to detect underground structures by means of the disturbance they produce at the surface in the earth gravitational field. It also aimed at measuring subsurface density variation, determine subsurface geometry, estimate depth to basement and distinguish between different rock types. Large scale studies of the crust employ gravity surveys. In these differences, the densities of subsurface rocks, basement topography, sedimentary basins along their tectonic architecture, and regional groundwater exploration are mapped using measurements of the earth's gravitational field (Sultan *et al*., 2009). Gravity method is used in structural interpretation of sedimentary basins because of their better spatial resolution (Kearey *et al*., 2002). The effectiveness of gravity survey depends on the existence of a significant density contrast between altered rocks or structures and their host rocks. Moreover, gravity survey not only reflects the shape of major granitoids, but also a correspondence between the tectonic lineaments and regional fault system (Ismail *et al.,* 2001).

EDITOR-IN-CHIEF
Prof. W. F. HILL [MALAWI]

Many gravity maps over Nigeria including the theoretical gravity map, absolute gravity map, and Bouguer gravity anomaly map to the geoid have been published (Akintoye *et al*., 2023). However, the literature review shows that there is limited gravity geophysical survey carried out in the study area, hence, the initiation of this study work is to understand and characterized the structural styles and regional trends of the Earth sequence beneath the study area and structures containing hydrocarbons. The aerogravity method is a geophysical technique used to measure the Earth's gravitational field from an aircraft. The gravitational field of the Earth is measured using the gravimeter, along flight line, typically high latitude. Datasets from gravitational investigations are processed to remove noise, correct for instrument drift, and account for terrain effects. The aerogravity method is relevant for identifying potential hydrocarbon- bearing structures in Sokoto Basin by mapping basement structures and sedimentary thicknesses. These method helps in delineating basins and structures where hydrocarbons might be trapped. By analyzing gravity variations, it can reveal subsurface density variations, which can indicate the presence of sedimentary basins and potential structural traps or hydrocarbons. Aerogravity survey are used to map the depth and structure of the basement rock beneath the sedimentary basin. This is crucial because the basement's structure can influence the formation of traps for hydrocarbon. The method helps in estimating the thickness of the sedimentary layers within the basin. Thicker sedimentary sequences are often associated with greater potential for hydrocarbon generation and accumulation, as they can provide the necessary source rocks and reservoir rocks. By analyzing gravity anomalies, the aerogravity method can help identify faults, folds, and other structural features that can act as traps for hydrocarbon. Aerogravity data can be integrated with other geophysical data such as aeromagnetic data, to provide a more comprehensive understanding of the subsurface and improve accuracy of hydrocarbon perspectivity assessments (Onyeche *et al*., 2023).

Litho-structural evaluation and depth to basement studies in the Sokoto Basin are critical for identifying sedimentary thicknesses over 2km and deep-seated structural traps (faults, grabens) using techniques like Euler deconvolution enabling targeted hydrocarbon and solid mineral exploration reducing exploration risks, and enhancing Nigeria's economic diversification and energy security (Kamurejina *et al.,* 2019; Ishola *et al.,* 2026). Litho-structural evaluations and depth to basement studies in the Sokoto Basin have high and varying implications. It involves Basin configuration which defines the geometry of lullemmeden basin, identifying areas with thick sedimentary sequences suitable for oil and gas accumulation; Structural mapping delineates faults, fractures, and lineaments which are essential as traps for hydrocarbon accumulation and conduits for hydrothermal mineralization; hydrocarbon maturation determines if the sedimentary column is deep enough (typically > 2km) for thermal maturation with studies indicating high potential in certain central parts. There are lots of benefits and prospects in carrying out Litho-structural evaluation and depth to basement studies in the Sokoto Basin, this includes

EDITOR-IN-CHIEF
Prof. W. F. HILL [MALAWI]

optimized exploration, mineral prospecting, and hydrogeological insights (Kamurejina *et al.,* 2019; Likkason et al., 2024; Ishola *et al.,* 2026). In optimized exploration, high-potential areas (e.g areas around Dogon-Marke) can be narrowed down for detailed seismic surveys, reducing costs associated with speculative drilling; in mineral prospecting, anomalous zones associated with mineralized veins and igneous intrusions that could aid in the search for solid minerals like gold and base metals; hydrogeological insights, it provides information on groundwater potential within sedimentary layers. Economic significance of Litho-structural evaluation and depth to basement studies in the Sokoto Basin includes energy security which could significantly add to Nigeria's known hydrocarbon reserves outside the Niger-Delta area; if fosters regional development through the development of new infrastructures and industries in Northwestern Nigeria thereby promoting the economic exploitation of mineral deposits, generating employment opportunities and boosting local economies (Megawata *et al.,* 2025).

The integration of high-resolution aeromagnetic data ensures a better understanding of the subterranean geology of the Sokoto basin. This crucial data reduces the financial risk of exploration and guides government and private investors toward the most promising areas for resources, fostering national development. The proposed exploration work and consequent discovery of hydrocarbons in the Sokoto Basin and Northern Nigeria presents significant economic opportunities which may include over three billion dollars in initial investments, diversification of oil producing beyond the Niger-Delta, job creation, and increased government revenue. These discoveries enhance national energy security, promote regional industrialization through gas supply, and strengthen Nigeria's position as a major oil producer in Africa. The proposed exploration work and exploitation outcomes of hydrocarbons will go a long way in providing both national and international/regional economic benefits; the national economic are production diversification and security by which the reduction in reliance on the Niger-Delta minimizes risks associated with pipeline vandalism and operational vandalism and operational disruptions in that region; creation of investment influx just as the Kolmani River II project in the Upper Benue Trough which attracted over three billion dolllars in investments thereby attracting foreign and local capital to the region; Job creation and regional development where exploration, development, and eventual production create jobs, reduce poverty, and trigger infrastructural development in Northern part of Nigeria; industrialization via Gas production where inland gas exploration allows for the creation of industrial clusters, providing feedstock for fertilizer plants and fuel for domestic power generation for industrial clusters; revenue boost due to increased exploration and production help increase national revenue which is vital as the oil sector contributes roughly 60% of government revenue. The increased national oil reserves, massive foreign investment, enhanced regional development and employment opportunities as these inland basins reduce reliance on Niger Delta oil, boost domestic refining capacity and foster energy security thereby enhancing Nigeria's position in the global energy market.

EDITOR-IN-CHIEF
Prof. W. F. HILL [MALAWI]

The international/regional benefits among others are improved energy security as the discovery boosts Nigeria's capacity to meet its OPEC production quota (e.g., 1.7 to 1.8 million barrels daily) and potentially exceed them; attraction of Foreign Direct Investment (FDI) since the new frontier basins will offer opportunities for international oil companies to invest new, under-explored regions thereby boosting Nigeria's daily output, assisting in meeting global energy demand and potentially impacting oil prices contributing to global energy security; emergence of regional economic growth where the development stimulates industrial growth, potentially making Nigeria a hub for petrochemical products in West Africa. Also, the investment opportunities will attract international investors to new frontier basins, signaling potential for exploration in other under-explored African areas (Ajiya, 2023; Darkkah *et al.,* 2025). Alongside with the Gongola Basin, the Sokoto Basin holds promise, with geological studies indicating dark shales and limestones as promising source rocks, the potential for commercial quantities of hydrocarbons including potential for 808 million barrels of oil equivalent in certain areas, providing a foundation for future energy security (Obaje *et al.,* 2020; Ajiya, 2023; Darkkah *et al.,* 2025). Obaje *et al.* (2020) investigated the petroleum potentials of Sokoto basin in Northwestern, Nigeria using geophysical method of Aeromagnetic data interpretation to determine depth to basement configuration alongside geochemical analysis to reveal subsurface rocks in the area. Source rock average thickness of 50m with basin area 60,000kmsq, TOC of 7.5wt% and HI of 212mg HCI g TOC and charge modelling of indication of 808.10 million barrel of oil were discovered through the study. The area was found to contain ground potential source rock while Abubakar and Likasson (2022) characterized regional trend of the earth sequence system of the Sokoto basin, north West Nigeria using potential field gravity techniques namely theoretical model, gravity data reduction, geological framework analysis, bouguer reduction density among others for the purpose of revealing the structural styles and regional trends of the subsurface formation in Sokoto. The bouguer map revealed high characteristics features of strong positive oval shape of causative body anomaly of (> -14.0mGal) trending E-W while a number of gravity minima (-43.31mGal) and maxima (-39.54mGal). The anomalous features show revealed negative outcomes as well as the lineament patterns are initially oriented in the NW-SE, ENE and E-W trends. Several authors have also applied aerogravity method of geophysical prospecting in other locations of the world; Ndougsa-Mbarga *et al.* (2007) investigated the Mamfe sedimentary basin, which is linked to the hydrocarbon-rich Benue Trough and the deeper Western sub-basin near Ekok and Agbakem; Okpoli and Akingboye (2019) in Igbabi area in Northwestern Nigeria. Akintoye *et al.* (2023) analyzed gravity data over Nigeria North-Central Basement Complex, focusing on Kaduna and Kastina states including an extension of the Ifewara-Zungeru fault zone; Nwankowo *et al.* (2012) conducted a study on the petroleum potential of the Chad Basin, Nigeria using heat flow and gravity data; Fyhn *et al.* (2010) investigated the geological evolution and petroleum potential of the underexplored Vietnamese margin comprising of several sedimentary

EDITOR-IN-CHIEF
Prof. W. F. HILL [MALAWI]

basins, including the Son- Hong, Khanh, Malay-Tho Chu, and Phu-Quoc basins; Kasidi and Yusuf (2019) studied the hydrogeological and petroleum potential of the Nigeria sector of the Chad Basin part of the West and Central African Rift system; Adewumi and Salako (2018) employed high-resolution aeromagnetic data to delineate mineral potential zones in parts of Nasarawa state, North Central, Nigeria including the basement complex in areas like Wamba and sedimentary regions like Lafia and Doma host industrial minerals; Tawey *et al.* (2020) applied aeromagnetic data to assess sun-surface and solid mineral potential in North Central Nigeria; Emujakporue *et al.* (2017) investigated the basement morphology and tectonic lineaments of the parts of the Sokoto Basin, Northwestern Nigeria; Ogbodu *et al.* (2025) examined the sediment thickness distribution and depth of the Ikom Basin, southeastern Nigeria; Ekwueme *et al.* (2018) analyzed aeromagnetic anomalies in Idah and Angba, North Central Nigeria; Salawu *et al.* (2020) interpreted aeromagnetic data to map subsurface structures in Ibi, Middle Benue, Nigeria; Osinowo and Olayinka (2013) explored the basement topography of the Ijebu-Ode transition zone on southwestern Nigeria using aeromagnetic mapping; Casas *et al*. (2016) conducted a study on the application of gravity methods for delineating diapiric structures in northeast Spain, highlighting new challenges in the field focusing on the South Pyrenean Central Unit, an area characterized by the presence of Triassic and Oligocene evaporites related to thrust-and-fold systems; Falufosi and Osinowo (2021) conducted a comprehensive review of the geology and hydrocarbon potential of the Nigerian sector of the Dahomey Basin, emphasizing the basin's tectonic evolution, sedimentary history, and petroleum systems. They highlight the structural complexity of the basin, which resulted from basement subsidence, block faulting, and subsequent sedimentation from the Early Cretaceous onward. Their study aligns with previous works by Omatsola and Adegoke (1981), who classified the basin's stratigraphy into the Abeokuta Group, consisting of the Ise, Afowo, and Araromi Formations. The authors also discussed hydrocarbon generation on the published literature, noting the presence of proven offshore hydrocarbon fields and onshore deposits of heavy oil and tar sands with Billman (1992) supporting this by emphasizing the role of the basin's structural framework in hydrocarbon entrapment; Obaje *et al.* (2020) conducted a study on the geology and potential petroleum system of the Bida Basin in Central Nigeria emphasizing its stratigraphy, structural framework, and hydrocarbon potential. Their research revealed that the basin contains thick sedimentary sequences, with the central portions being the most prospective for hydrocarbon accumulation. The authors identified the Kudu Shale in the Northern Bida Basin and the Ahoko Shale in the Southern Bida Basin as the primary source rocks, exhibiting significant organic richness but requiring deeper burial for maturity. The findings of the authors aligned with the previous studies by Ojo and Ajakaiye (1989), who used gravity and magnetic data to establish the basin's structural trends, and by Udensi and Osazuwa (2004), who determined sediment thickness variations using spectral analysis; Akande *et al.,* (2005) further supported these findings by conducting geochemical studies, indicating

EDITOR-IN-CHIEF
Prof. W. F. HILL [MALAWI]

that organic matter in the source rocks was immature to marginally mature. The study highlighted the potentials of the Bida Basin as a hydrocarbon-bearing province, with aeromagnetic and seismic interpretations suggesting the presence of sub-basins that could serve as hydrocarbon traps. Arogundade *et al*. (2020) conducted a study on the analysis of aeromagnetic anomalies in parts of the Chad Basin, Nigeria; their findings aligned with the previous studies by Nwankwo and Ekine (2009), who estimated geothermal gradients in the Chad Basin, and Awoyemi *et al.,* (2016), who mapped basement faults using aeromagnetic data. Additionally, Petters and Ekweozor (1982) highlighted the basin's favorable geochemistry for hydrocarbon generation. These studies collectively emphasized the Chad Basin's structural complexity and its potential for hydrocarbon accumulation.

The aim of this study is to delineate and identify geological characteristics for hydrocarbon and solid minerals potentials using high-resolution airborne gravity data in parts of Sokoto Basin via the generation and interpretation of Bouguer anomaly map to analyze and interpret subsurface geologic structures in Sokoto basin, Regional Anomaly Map to analyze and interprets the regional field caused by long wave gravity anomalies that are associated with deep seated basement features from the observed Bouguer Anomalies. Residual Anomaly Map to determine the local field of interest (shallow structures) arising from shorter wavelength anomalies, first vertical derivative map to analyze and interprets shallow subsurface structural features along vertical directions, first horizontal derivative map to analyze and interprets the edges and boundaries of identified causative bodies and structures along different directions. Analytical signal map to analyze the total field gradient for defining the edges and boundaries of geologically anomalous density distributions while application of Euler Deconvolution technique was undertaken for depth estimation and structural evaluation; to determine the depth to the top of gravity sources as well the trends and dimensions of anomalous sources.

Location and Accessibility

The study area is located within the Sokoto basin, which is Nigerian sector of the larger lullemmenden basin which spans across parts of Algeria, Benin Republic, Niger Republic, and Libya (Obaje *et al.,* 2013). The Sokoto Basin, also known as the lullemmeden Basin, spans northwestern Nigeria and extends into Niger and other neighboring countries. The study area lies within the latitudes 4° 12′0″ E and 4° 48′0″ E and longitudes 11° 48′0″ N and 11° 12′0″ N. The road is accessible by major and minor roads as well as footpaths linking to the major and minor roads, making it easier for surveying.

Relief and Drainage

The topography map of the study area (Figure 1) was obtained from the digital elevation model (DEM, 2006) and covers approximately 48,400km$^{2.}$ The study area is predominantly a gentle undulating plain with an average elevation varying from 250- 400m above sea

EDITOR-IN-CHIEF
Prof. W. F. HILL [MALAWI]

level. The plain is occasionally interrupted by low mesas and other escarpment features (Kogbe, 1979).

Climate and Vegetation

The study area enjoys tropical continental type of climate. Mean annual rainfall is about 800 to 1000mm while the mean annual temperature ranges from 26.5 to 40°C. Night temperatures are generally low. The highest temperature occurs between April and July, the lowest in August (during rainy season). It's geographically located in the semi-arid with a zone of savannah-type vegetation as part of the sub-Sahara Sudan belt of West Africa.

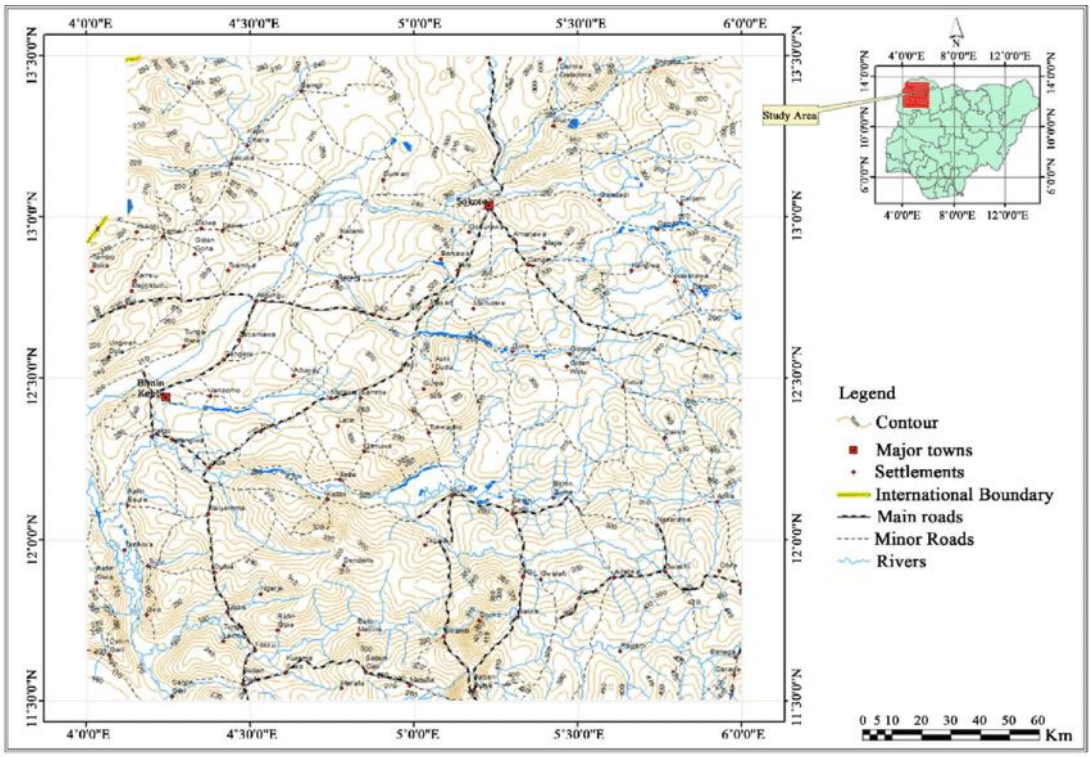


Figure 1: Topographical map of the study area (analyzed from Digital Elevation Model (DEM, 2006; Kamureyina *et al.*, 2019)

Physiography and General Geology of the Study Area

The sedimentary basins in northwestern Nigeria principally include Illo and Gundumi Formations (Cretaceous): Found in the Sokoto basin, these formations consist of sandstones and conglomerates, representing fluvial deposits (Kogbe, 1979; Kogbe, 1989). Also, the occurrence of Rima Group (Paleogene) which includes the Dukamaje, Taloka, and Wurno formations, characterized by marine shales and sandstones (Petters, 1978). The study area is part of Sokoto basin which falls within Kebbi state. Sokoto state is a

EDITOR-IN-CHIEF
Prof. W. F. HILL [MALAWI]

large, elongated sedimentary basin that underlies much of the Northwestern Nigeria and extends into the eastern portions of Niger Republic (Figure 2). Kebbi state occupies a significant portion of the western Sokoto basin. The sediments of the lullemmeden Basin were thought to accumulate during four main phases of deposition (Figure 2). The Illo and Gundumi Formations (made of grits and clays) unconformably overlie the pre-Cambrian Basement Complex. This is the so-called Pre-Maastrichtian 'continental interclaire' of West Africa (Obaje *et al*., 2013). Next on the succession is the Maastrichtian (66–72 Ma) Rima Group (consisting of mudstones and friable sandstones) (the Taloka and Wurno formations) separated by the fossiliferous, calcareous and shaley Dukamaje Formation overlies the Illo and Gundumi Formations unconformably (Kogbe, 1979). The Dange and Gamba Formations (mainly shales separated by the calcareous Kalambaina Formation constituting the Paleocene) (56–66 Ma) Sokoto Group overlie the Rima Group (Kogbe, 1979). The sequence cover is the Gwandu Formation of the Eocene (33–56 Ma) age forming the continental terminal (Kogbe, 1981). The sediments dip gently and thicken gradually towards the northwest with maximum thicknesses attainable towards the border with Niger Republic. Considering the stratigraphic successions in the Nigeria sector of lullemmeden basin (Sokoto basin) (Table 1). So, within Kebbi state, the Sokoto basin encompasses the Gwandu Formation, part of the Sokoto group, and the Rima Group. Gwandu Formation is the youngest Paleogene formation present in the Sokoto sector of the larger lullemmeden basin. The Gwandu formation is found in the western part of the Sokoto basin which occupies most parts of Kebbi state. The Gwandu Formation along with other formations in the Sokoto basin have drawn attention from geoscientists and petroleum industry due to the intensified petroleum exploration efforts in the inland basins. Although there are other states in the North-West Geopolitical zone like Jigawa, Kaduna, Kano, Katsina and Zamfara. Aside from Sokoto state, Kebbi state is the only state that is primarily located within the Sokoto basin bordering Sokoto state to the North while Sokoto state is partially located within the Sokoto basin bordering Kebbi state to the West and South and Zamfara to the South and East. Kebbi state is indeed typically characterized by the Gwandu Formation, a sedimentary deposit within the Sokoto basin and is considered the youngest in the Sokoto basin, a region known in terms of geological context to be extensive sedimentary deposits consisting of continental lacustrine sediments (Figure 2). The Gwandu Formation, consists of locally indurated, interbedded, thick grey, brownish black and red mudstones, a continental sequence of grits and clay, including interbedded mudstones alongside with fine to very coarse-grained white and brown quartz sand with individual mudstone sections reaching over 60m thick while sand sections are less than 35m thick. The Gwandu Formation is particularly prominent in and around Birnin Kebbi, the state capital with exposures scattered throughout the metropolis and its outskirts. Aside from the sedimentary

EDITOR-IN-CHIEF
Prof. W. F. HILL [MALAWI]

deposits, the basement complex region is composed of very old volcanic and metamorphic rocks such as granite, schist, gneisses and quartzite whose ages range from cretaceous to Eocene. In terms of Depositional Environment, the Gulma sandstone member of the Gwandu Formation is a texturally and mineralogically sub matured sediment, suggesting a marginal marine setting of a tidal and tidal shelf deposition. Economically, the region possesses notable mineral deposits, including gold deposits that are found in schist belts of Birnin Gwari, Maru, and Anka (Garba, 2002). Limestone and Phosphate deposits that are abundant in the Sokoto Basin, particularly the Kalambaina Formation and Lead-Zinc and Copper deposits occurring in sedimentary sequences and veins in the basement complex (Figure 2).

Table 1: Stratigraphic Succession in Sokoto Basin (Obaje, 2009)

Age	Type/ Group	Formation	Sediment type	Remark
Eocene	---------	Gwandu	Continental	Continental terminal
Paleocene	Sokoto Group	Gamba Kalambaina Dange	Marine Marine Marine	------- ------- -------
Maastrichtian	Rima Group	Wurno Dukamaje Taloka	Continental Marine Continental	------- ------- -------
Pre-Maastrichtian		Gundumi-Illo	Continental	Continental interclaire
Pre-Cambrian	Basement Complex rocks			

The location for the lithostratigraphic exposure was observed at Dukku hill near Dukku river very close to the bridge. The total thickness of exposure is about 21.83m consisting of 2.6m thick of variegated and laminated silty clay, overlain by 1.03m thick, bulky red patched silty clay stone and so on. While other range of sediments types from silty clay to Ironstone also be observed at Dukku hill (Obaje, 2009).

Local Geology of the Study area

Aida is situated within the Maiyama Local Government Area of Kebbi State, Northwestern Nigeria. The geology of Kebbi State is characterized by a combination of sedimentary deposits from the Sokoto Basin and Precambrian basement complex rocks. Approximately, 50% of the state is underlain by thick sequences of sedimentary deposits from the Sokoto Rima-Basin while remaining areas consist of Precambrian basement

EDITOR-IN-CHIEF
Prof. W. F. HILL [MALAWI]

complex rocks. These formations of sedimentary compositions comprising of Illo and Gundumi formations at the base followed by the Taloka, Dukamaje, Wurno, Dange, Kalambaina, Gamba, and Gwandu formations are found to consist of sandstones, limestones, laterites. Siltstones, meta-conglomerates, shales and clays (Figure 3). Majidi is also located within the Maiyama Local Government Area of Kebbi State, Northwestern Nigeria and equally characterized by the Precambrian basement complex rocks and sedimentary formations associated with the Sokoto Basin. The basement complex rocks in Kebbi State include granite gneiss, migmatitic augen gneiss, and medium to coarse-grained biotite; these formations are part of the Precambrian crystalline basement complex that underlies the southeastern portion of the state. The sedimentary formations of the Sokoto basin which cover approximately 50% of Kebbi State consist of various deposits ranging from the cretaceous to Eocene; these include the Illo and Gundumi formations (comprising pebbly grits, sandstones, and clays), the Rima group (comprising of mudstones and siltstones) and the Gwandu formation (characterized by massive clays interbedded with sandstones). Kashe hill is located in the Bagudo Local Government Area of Kebbi State, Northwestern Nigeria as part of the regional geological framework which includes both Precambrian basement complex rocks and sedimentary formations associated with the Sokoto Basin. The basement complex comprises of ancient crystalline rocks such as granite-gneiss and migmatites while the sedimentary formations consist of sandstones, shales, and clays deposited during the cretaceous and tertiary periods. Farin-Ruwa is located in the Gulbin-Kuka district of Fakai Local Government Area of Kebbi State, Northwestern Nigeria and lies within the geological framework of the region. The basement complex comprises ancient crystalline rocks such as granite gneiss, migmatites, and schists, indicative of a complex metamorphic history while the sedimentary formations from the cretaceous period consist of sandstones, siltstones and clay deposits. Since Kebbi State is known to host various mineral resources including clay deposits; a section of kaolinitic clay within the formation termed" pistolitic clay member" has been described in the region. These clays are relatively rich in Kaolin with a small excess of alumina and less than 1% iron oxides (Ishola and Akinyemi, 2025). Tunga-Namaruwa lies within a region characterized by diverse geological formations. Since the geology of Kebbi state is predominantly divided between the Precambrian basement complex in the south and south-east, and younger sedimentary rocks in the north. The basement complex of this area comprises ancient volcanic rocks such as granites, schists, gneisses, and quartzites. In contrast, the sedimentary formations include the Gwandu, Illo, and Rima groups, with ages ranging from the cretaceous to the Eocene periods. The Gwandu group consists of massive clay interbedded with sandstone while Illo and Rima groups are composed of pebbly grits, sandstones, clays, mudstones and siltstones. Koko/Besse area is located within Koko/Besse Local Government Area of Kebbi

EDITOR-IN-CHIEF
Prof. W. F. HILL [MALAWI]

State encompasses diverse geological formations primarily characterized by rocks that are associated with the Sokoto Basin. The region's geology includes Illo and Gundumi formations consisting of pebbly grits, sandstones and clays. These sedimentary sequences were deposited during the cretaceous to Eocene periods. Geophysical studies have identified areas within Koko/Besse with low magnetic susceptibility values, suggesting the presence of sedimentary rocks like sandstones, siltstones, clay/shales, limestones and laterites; these findings are consistent with the geological composition of the Sokoto Basin. Tunga-Atto is located within the Koko/Besse Local Government Area of Kebbi State which lies within a region characterized by sedimentary formations associated with the Sokoto Basin. These formations, primarily dating from the cretaceous to Eocene periods including Illo and Gundumi formations consisting of pebbly grits, sandstones, and clays as sedimentary sequences. Geophysical studies in the southern part of Kebbi State have identified areas with low magnetic susceptibility values suggesting the presence of sedimentary rocks that are also consistent with the geological composition of the Sokoto Basin. Gidan-Jero is located in the Kangi District of Fakai Local Government Area whose geology is being influenced by the Precambrian Basement Complex comprising of ancient crystalline rocks such as granites, schists, gneisses, and quartzites. Geophysical assessments have identified structures within this area that may host gold mineralization. Techniques like aeromagnetic data analysis have been employed to delineate these structures revealing lineaments trending in the NE-SW directions which are associated with potential mineralized zones (Ishola and Akinyemi, 2025). Rorukos Hill is located in the Wasagu/Danko Local Government area of Kebbi State situated within the Zuru-Schist Belt, a component of the Nigerian Basement Complex. The region is predominantly characterized by metamorphic rocks such as schists, gneisses, and quartzites which have undergone multiple deformation and metamorphic events. The Zuru-Schist Belt is also noted for its potential mineral resources including gold mineralization associated with quartz veins and other structural features (Obaje *et al*., 2013). Maidiji is also located in the Wasagu/Danko Local Government area of Kebbi State situated within the Zuru-Schist Belt; a segment of the Nigerian Basement Complex. This region is predominantly composed of Precambrian metamorphic rocks including schists, gneisses, quartzites and migmatites; these formations have undergone multiple deformation and metamorphic events contributing to the area's complex geological history. Past geological studies in the southern part of Kebbi State have identified significant structural features such as faults and fractures trending in the NE-SW direction. These structures are associated with potential gold mineralization particularly within the basement complex regions encompassing areas like Wasagu/Danko. The presence of rock types such as granite, rhyolite, biotite gneiss, meta-conglomerate, quartz-mica schist, migmatite and gneiss further supports the areas mineralization potential. Sakaba is

EDITOR-IN-CHIEF
Prof. W. F. HILL [MALAWI]

located in the southern part of Kebbi state. It is geologically situated within the Zuru-Schist Belt, a component of the Nigerian Basement Complex. The region is predominantly characterized by metamorphic rocks such as mica schists, quartzites, amphibolites and gneisses; these formations are indicative of a complex geological history involving multiple deformation processes and metamorphic events.

Hydrogeology of the Study Atea

The hydrogeology of Kebbi State portion of the Sokoto Basin is characterized by a mix of cretaceous tertiary sedimentary aquifers and Precambrian Basement Complex rocks, supporting a multi-aquifer system. The sedimentary portion (~50% of the state) consists of thick sequences including the Ilo, Rima, and Kalambaina formations, which dip and thicken towards the northwest. Groundwater in the region is generally of good quality, but the area faces high evapotranspiration and increasing reliance on groundwater to mitigate drought (Megawata et al., 2025). The geologic setting consists of two main hydrogeological units namely the sedimentary basin at the Northwest of Kebbi, part of the lullemmeden Basin containing sedimentary deposits that hold major aquifers and the Basement complex at the South/East Kebbi that is composed of crystalline rocks including plutonic granite, gneiss, and schist where groundwater is limited to fractures and weathered regolith (KSG, 2014; Walracuens et al., 2018; Ahmed et al., 2019; Ahmed et al., 2020; Tanko et al., 2020) (Figure 2). The Kebbi part of the basin relies on several primary aquifers with Birnin Kebbi primarily utilizing the Gwandu and Illo formations. Gwandu formation at the continental terminal is composed of two main aquifers (upper and lower), it is the most prominent aquifer in the western Sokoto Basin ranging from 15 to 75m; Illo formation is hydraulically often continuous with the Rima Group and it serves as a significant aquifer particularly around Birnin Kebbi; Rima Group (Wurno formation) is a reliable, moderate-output aquifer consisting of sandstones; Kalambaina formation serves as a limestone unit that acts as a perched aquifer, suitable for shallow, small-scale domestic water (Waliu *et al.,* 2019). In terms of hydrogeological characteristics, the study area is primarily recharged through direct infiltration of rainfall and runoff on the outcrop areas (Figure 2). The artesian conditions reveal that the western part of Kebbi, particularly near the border with Niger Republic, the Gwandu formation shows confined artesian conditions due to covering lignite and clay layers. Generally, the groundwater flows follow the dip of the formations, thickening and flowing towards the Northwest with the static water levels varying from 2.3m to 30m in the basement complex areas to deeper levels in the sedimentary upland regions (Oteze, 1991; Umako, 1993; Nura *et al.,* 2018; Kwaya *et al.,* 2019; Kwaya *et al.,* 2020). In terms of production, the yields in the basement complex area of Southern Kebbi are lower with potential to produce approximately 14.67 gallons per second (gps) from average borehole depths of 37.49m. in terms of groundwater quality

EDITOR-IN-CHIEF
Prof. W. F. HILL [MALAWI]

consideration, groundwater in the Kebbi part of the Sokoto Basin is generally suitable for domestic, agricultural, and industrial use, although it exhibits significant spatial variability (Freeze and Barber, 1965; Oteze, 1976; Edwards *et al.,* 1991; Umar, 1998; Sayad *et al.,* 1998; IOAHIC, 1999; UNICEF, 1999; BGS, 2003; Maduabuchi et al., 2003; Adelana and MaCdonald, 2008; Tijani, 2008; UNEP, 2010; Al-Amin, 2013). The water type is predominantly Ca-Mg-HCO_3 or Ca-Cl, indicating high hardness in some areas, the quality metrics is mostly excellent good, though some areas in Argungu, Birnin Kebbi, and Kalgo show high TDS and Iron (Fe^{3+}) concentrations that exceed WHO standards. The pollution levels in some areas reveal high Nitrate (NO_3-) levels suggesting potential contamination from agricultural or surface runoff (Anderson *et al.,* 1976; Umako, 1993; FMWRRD, 1995; Adelana *et al.,* 2005; Adelana *et al.,* 2006; WHO, 2011; Emere and Dibal, 2013; Joseph, 2015; NSDWQ, 2015; Waliu *et al.,* 2019; Tanko *et al.,* 2021; Ayobami and Theophillus, 2022). Certain hydrogeological challenges have been reported that have been attributed to high potential evapotranspiration where the semi-arid climate (annual rainfall <600mm in some northern parts) causes high water loss and a reliance on deep aquifers; water scarcity despite having rich aquifers, localized shortages occurrence due to poor borehole construction and high reliance on few productive aquifers; aquifer contaminations where shallow hand-dug wells are susceptible to faecal coliform contamination (Alagbe, 2006; Dankwo and Lar, 2013; NSDWQ, 2015; Elumali *et al.,* 2017; Ette et al., 2017; Arseni *et al.,* 2018; Admalla, 2018; Ibrahim *et al.,* 2020; Atunuga *et al.,* 2020; Asiwaju Bello *et al.,* 2020; WHO, 2021; Otlaadosa *et al.,* 2022; Adetona *et al.,* 2024; Usman *et al.,* 2024).

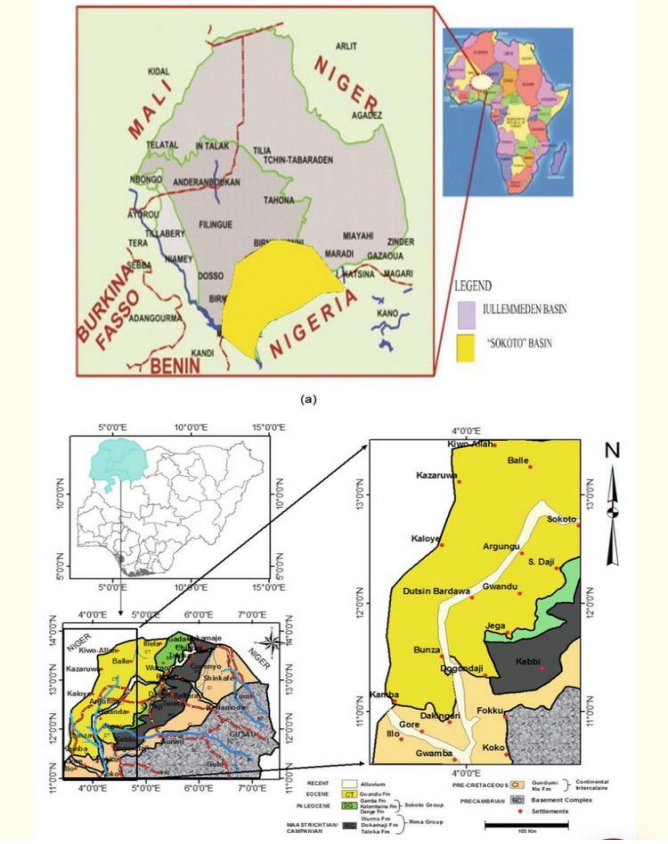


Figure 2: Geological Map of Nigeria showing the Study area within Sokoto Basin (Kogbe, 1976; modified by Ishola and Akinyemi, 2025)

EDITOR-IN-CHIEF
Prof. W. F. HILL [MALAWI]

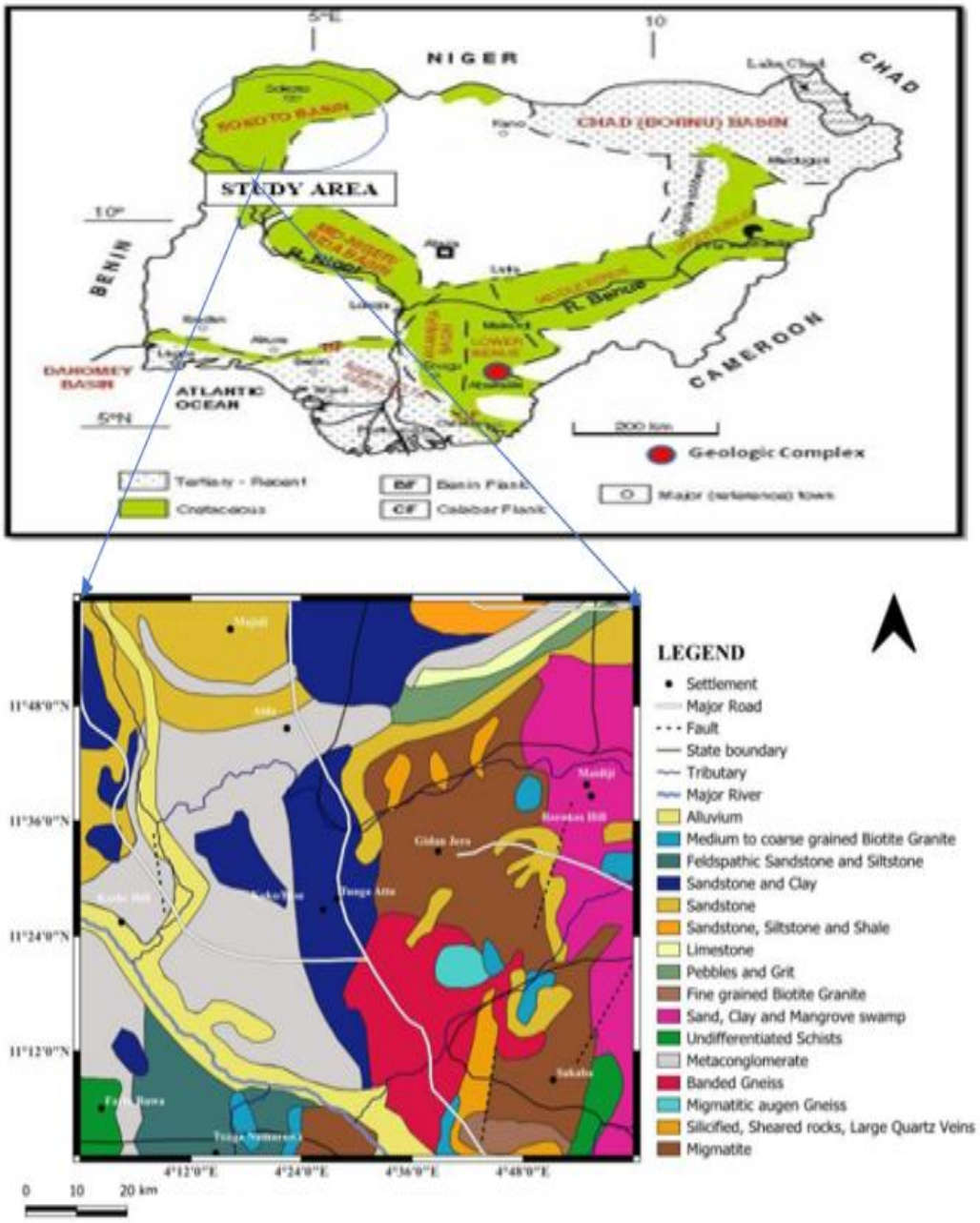


Figure 3: Local Geology of the Study area within Sokoto Basin (Ishola and Akinyemi, 2025)

Concept of Gravity and Rock Density

The gravity method is a geophysical method or techniques used to measure variations in the Earth gravitational field at the surface whether on the land, sea or in the air. It is a passive method, in the sense that no artificial energy is required to acquire the data. The strength of the gravitational field is directly proportional to the mass and density of the

subsurface materials (Wilcox, 1989; Onyeche et al., 2023). Gravity value changes as objects move from one position on the earth's surface to another. As a result, gravity measurements provide information on the densities of underlying rocks, which can be used to better understand subsurface geology. Since there is a wide range in density among rock types, geologists can make inferences about the distributions of strata. The success of this method is dependent on the different bulk densities (mass) of the earth materials which cause variations in the measured gravitational field. The depth, geometry, and density that can cause the gravity field variations can then be determined using a variety of analytical and computational methods. It helps in identifying subsurface structures by detecting density variations beneath the surface (Phillips et al., 1998). It is based on the principle that different subsurface materials have varying densities, which causes slight changes in gravitational attraction. By analyzing these variations, geophysicists can infer the presence of geological structures such as faults, mineral deposits, oil reservoirs, and underground cavities. This method is widely used in mineral and hydrocarbon exploration, geotechnical engineering, and environmental studies. It is particularly valuable because it is passive, non-invasion technique that does not require the introduction of energy into the ground, unlike seismic or electromagnetic methods. Since gravitational acceleration is influenced by mass distribution beneath the surface, gravity surveys help map subsurface density contrasts. The data collected is often processed and corrected for various factors such as terrain, elevation, and instrument drift to produce accurate gravity anomaly map. These maps serve as essential tools in understanding subsurface geology and making informed exploration decisions. The gravity method is based on two laws derived by Sir Isaac Newton in 1687 namely law of Gravitation and his second law of motion. The universal law of gravitation states that the force of attraction between two bodies of known mass is directly proportional to the product of the two mass and inversely proportional to the square of the distance between their center of mass while his second law of motion states that the rate of change of momentum of a body, is directly proportional to the force applied and this change of momentum takes place in the direction of the applied force. The universal gravitational law according to Newton, can be expressed in equation 1.0 as

$$\vec{F} = -\widehat{e_r}\ \frac{Gm_1m_2}{r^2} \qquad (1.0)$$

Where $\vec{F}$ represents the gravitational force between two objects (Newtons, N); G represents the universal gravitational constant ($6.674\times10^{-11}\ m^3kg^{-1}s^2$); m_1 and m_2 which are the masses of the two objects (kg); $\widehat{e_r}$ is the unit vector in the direction of the position vector r of mass m_2 concerning mass m_1. r is expressed in equation 2.0 as

EDITOR-IN-CHIEF
Prof. W. F. HILL [MALAWI]

$$r = \frac{1}{|r|} \quad (2.0)$$

r in represents the distance between the center of the two objects (m). According to Newton's second law, it can be mathematically expressed in equation 3.0 as

$$F = Mg \quad (3.0)$$

Considering the gravitational attraction of a spherical, non-rotating, homogeneous Earth of mass M and radius R on a small mass M on its surface. It is relatively simple to show that the mass of a sphere acts as though it were concentrated at the centre of the sphere and by substitution in equation 1.0, the force of attraction is further expressed in equation 4.0 as

$$F = \frac{GM}{R^2} m = mg \quad (4.0)$$

Equation 4.0 is further simplified resulting to equation 5.0 as

$$g = \frac{GM}{R^2} \quad (5.0)$$

Where *F* is the force of attraction between bodies and M is the mass of the body. Force is related to mass by acceleration and *g* term in equation 5.0 is known as gravitational acceleration or simply, gravity. The weight of the mass is given by *mg*. on such an earth, gravity would be constant. However, the earth's ellipsoidal shape, rotation, irregular surface relief and internal mass distribution cause gravity to vary over its surface (Ishola and Akinyemi, 2025).

Theoretically, Gravity is universal. It applies everywhere, from small objects on Earth to large celestial bodies in space. Gravity weakens with distance, if the distance between two objects doubles the gravitational forces becomes one-fourth as strong (Ishola and Akinyemi, 2025).

Rock density varies significantly across different rock types due to factors such as mineral composition, porosity, and presence of pore fluids. The differences in rock density may influence the accuracy of gravity survey and some factors likely to affect density must be known which will therefore aid in the interpretation of gravity data. Ranges of bulk densities for a selection of different material types are listed in (Table 2). Also rocks at the surface are used to interpret gravity data because they may have undergone weathering or from boreholes, where they have suffered from hydraulic stress than when in in-situ are used to determine densities. To prevent misinterpretation of data, its crucial to

EDITOR-IN-CHIEF
Prof. W. F. HILL [MALAWI]

acknowledge that errors in density determination can significantly impact gravity survey analysis, particularly when examining gravity anomalies. In sedimentary rocks, density is influenced by porosity, the nature of pore fluids, density of rock matrix, composition, age and date of burial, tectonic processes. Higher porosity typically results in lower density, especially if the pores are filled with less dense fluids like water and hydrocarbons. Past research works have shown that under normal conditions, the density contrast between adjacent sedimentary strata is greater than 0.25Mg/m^3. Igneous rock typically has higher density than sedimentary rocks. The density of igneous rocks varies depending on their mineral composition, porosity, and degree of crystallization. Generally mafic (rich in iron and magnesium) rocks tend to be denser than felsic rocks (rich in silica and aluminum) (Ishola and Akinyemi, 2025).

Table 2: Densities of Common Geologic Materials (Telford *et al*., 1990)

Material types	Density range (Mg/m^3)	Approximate average density (Mg/m^3)
Sedimentary rocks		
Alluvium	1.96-2.00	1.98
Clay	1.63-2.60	2.21
Gravel	1.70-2.40	2.00
Loess	1.40-1.93	1.64
Silt	1.80-2.20	1.93
Soil	1.20-2.40	1.92
Sand	1.70-2.30	2.00
Sandstone	1.61-2.76	2.35
Shale	1.77-3.20	2.40
Limestone	1.93-2.90	2.55
Dolomite	2.28-2.90	2.70
Chalk	1.53-2.60	2.01
Halite	2.10-2.60	2.22
Glacier ice	0.88-0.92	0.90
Igneous rocks		
Rhyolite	2.35-2.70	2.52
Granite	2.50-2.81	2.64
Andesite	2.40-2.80	2.61
Syenite	2.60-2.95	2.77
Basalt	2.70-3.30	2.99
Gabbro	2.70-3.50	3.03

EDITOR-IN-CHIEF
Prof. W. F. HILL [MALAWI]

Material types	Density range (Mg/m^3)	Approximate average density (Mg/m^3)
Metamorphic rocks		
Schist	2.39-2.90	2.64
Gneiss	2.59-3.00	2.80
Phylite	2.68-2.80	2.74
Slate	2.70-2.90	2.79
Granulite	2.52-2.73	2.65
Amphibolite	2.90-3.04	2.96
Eclogite	3.20-3.54	3.37

Metamorphic rock density varies depending on parent rock composition, metamorphic grade, mineral composition and pressure conditions during metamorphism. On the other hand, metamorphic rock stands out for their abrupt and irregular density fluctuations, which can change significantly over very short distances distinguishing them from sedimentary and igneous rocks. It is worthy of note to state that gravity method of geophysical prospecting possesses better depth penetration compared to ground penetrating radar, high frequency electromagnetic method and DC resistivity techniques and is not affected by high conductivity values of near-surface clay rich soils (Mickus, 2004; Ishola and Akinyemi, 2025).

Corrections to Gravity Observation

Since the earth is slightly irregular oblate ellipsoid which connotes that the gravity field at its surface is stronger at the poles than the equator. The density distribution is irregular, particularly in an inelastic crust, which causes gravity to vary from expected value at the measurement position changes (Abubakar and Likkason, 2022). Therefore, the variations are expressed as gravity anomalies while the mapping of gravity anomalies gives an understanding of the structure of the earth. It is therefore essential to identify the reasons gravity varies and it can be corrected while adopting gravity method in exploring and characterizing regional trends of the subsurface (Keary et al., 2002; Adamu et al., 2021; Ishola and Akinyemi, 2025).

When measuring gravity data, raw gravity data must be corrected for various effects to obtain the true subsurface gravity anomaly. These corrections help account for geological, instrumental, and environmental factors that influence gravity measurements. The results of gravimeter measurements are gravity differences between an arbitrary reference point and a series of field stations (Figure 4). The measured values at each station have some influences which completely mask the desired effect if they were not removed. Therefore, before gravity measurement can be useful in possible indications of subsurface conditions (the observed gravity differences must be corrected

EDITOR-IN-CHIEF
Prof. W. F. HILL [MALAWI]

for those various large influences). The object of usable data is to remove the known effects caused by predictable features that are not of the target. The remaining anomaly is then interpreted in terms of subsurface variations in density; each known effect is removed from observed data.

Latitude Correction

The orientation of the earth and its equatorial bulge produce an increase in gravity with increase in latitude (Figure 4). Therefore, it becomes necessary to apply latitude correction for stations at different latitudes (Abubakar and Likkason, 2022). The value of gravity increases with the geographical latitude. With advance of earth's rotation, the earth's is not spherical but flattened at poles thus the distance factor causes the "g" value to increase from equator to pole by 6.6 Gals because the surface is closer to the centre at the poles. The correction for latitude is calculated by subtracting the theoretical gravity value from the observed gravity value using the International Gravity Formula. This correction is negative when moving north in the northern hemisphere or south in the southern hemisphere. It accounts for the increase in the gravity field from the equator towards the poles. For instance, at a latitude of 51°N, the local latitude correction is approximately 8 gravity units per kilometer. To ensure accurate gravity surveys with a precision of ±0.1 gravity units, the latitude of the gravity station needs to be known within ±10 meters, which is achievable with modern position- fixing techniques. Both the rotation of the earth and its slight equatorial bulge produce an increase in gravity with increase in latitude (Figure 3). The formula for latitude effect is the 1967 Gravity Reference System (GRS67) whose approximation is of the form displayed in equation 6.0

$$g_L(\theta) = 978{,}171.261\,(1 + 0.005278895 sin^2\,\theta + 0.000023462 sin^4\,\theta)\ \text{mGal} \ldots . 6.0$$

Where θ is the latitude of the station concerned in degrees.

Elevation Correction

Since gravity varies with height, it is necessary to correct all observation to a datum which is usually but not always sea level. The correction consists of two parts, the free air correction and Bouguer Correction (Keary *et al.,* 2002; Adamu et al., 2021; Ishola and Akinyemi, 2025).

The Free-Air Correction (FAC) which is centered on the basis of gravity response as it decreases with increasing elevation above sea level. The free air correction is the difference between gravity measured at sea level and at an elevation of h meters of the station with no rock in between. It can be expressed from the difference between the measured or absolute gravity of a station (g_{obs}), extrapolated from the reference

EDITOR-IN-CHIEF
Prof. W. F. HILL [MALAWI]

ellipsoid and correcting it for the free air effect. The final result of the free air anomaly is given in equation 7.0 as

$$\Delta_{gyA} = \Delta_{obs} - (g_{lat} - \frac{\delta g}{\delta s} h) \quad 7.0$$

Where $\frac{\delta g}{\delta s}$ is the vertical gradient and it is the station elevation above mean sea level in meters above and its value is 0.3086 Gal m^{-1}(3.086 g.u/m). In practice, this value l is the only value used after deriving equation 7.0; thus, assuming that the earth's is spherical and non-rotating. Therefore, FAC considers only the correction considers only elevation differences relative to a datum and does not take into account that the mass between the observation point and datum and does not take into account that the mass between the observation point and datum as the station were suspended in free-air, not lying or sitting on land; these serve as the reason that the correction termed as free-air correction ((Figure 5). In general, the datum used for gravity surveys is sea level and gravity decreases 0.3086 Gal m^{-1} (3.086 g.u/m) for every meter above sea level (3.086 g.u/m). A value of 3.086 g.u/m is accepted for most practical applications and is positive at elevations above sea level, and negative below. The free air correction varies slightly with latitude from 3.083g.u/m at the equator to 3.088g.u/m at the poles. It

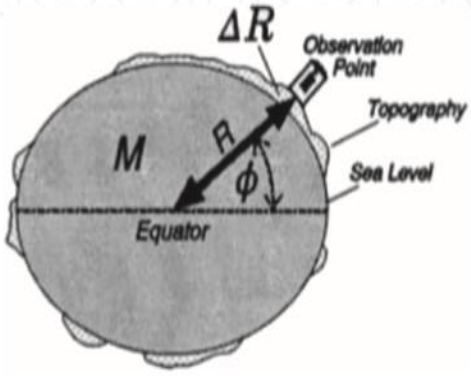


Figure 4: Earth rotation bulging at the equator (Abubakar and Likasson, 2022)

Bouguer Correction **is** the difference between the observed gravity and the theoretical gravity at any point on the earth corrected for the mass of materials between the point and the datum plane (Figure 4), its value *0.04188ρ*, where ρ is the density of the slab (Nettleton, 1976; Kayan, 2008; Telford *et al.,* 1998; Osazuwa, 1991; Abubakar and Likasson, 2022). Bouguer correction is applied in the opposite sense of free air; it is subtracted when the station is above the datum plane and vice-versa. Bouguer correction accounts for gravitational of the mass above sea-level datum plane and added when the station is below the datum plane (Figure 5). Bouguer correction accounts for gravitational of the mass above sea-level datum. The equation for Bouguer gravity at a point after all the necessary preceding corrections have been applied can be expressed in equation 8.0 and 9.0 as

EDITOR-IN-CHIEF
Prof. W. F. HILL [MALAWI]

$$g\,(B_{grav}) = g_{(obs)} - BC \qquad (8.0)$$

where BC is the Bouguer correction.

$$g\,(BA) = g\,(B_{grav}) - g\,(\text{Theoretical}) \qquad (9.0)$$

where *BA* is the Bouguer Anomaly.
Hence, the Bouguer anomaly is determined using the expression displayed in equation 10.0 as

$$g\,(BA) = g_{(obs)} - g_{lat} + \frac{\delta g}{\delta s} h - 2\pi\rho Gh \qquad (10.0)$$

Where πρ is the assumed crustal density value which is 2.67×10^{11} kgm^3 or Bouguer density and G is the universal gravitational constant. The term *2Gh* in the Bouguer correction represents the additional attraction exerted on a unit mass by a slab of rock material of density between a station and reference datum-mean sea level (m.s.1).

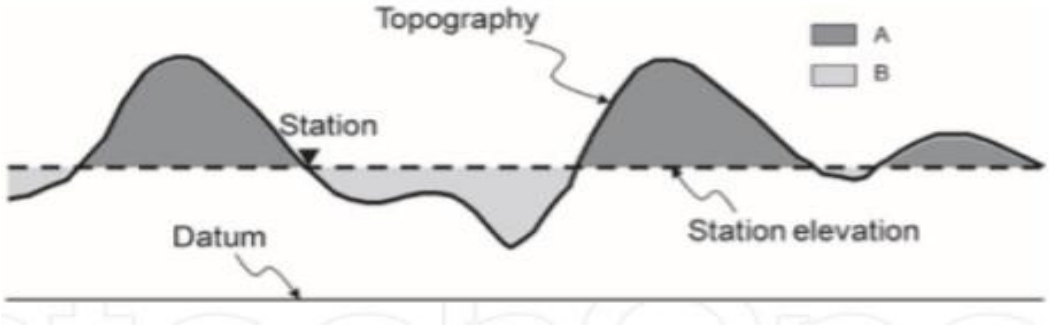


Figure 5: Field representation of Bouguer correction (Abubakar and Likasson, 2022)

Bouguer Gravity Anomaly

A bouguer gravity anomaly is the difference between the observed acceleration of an object in free fall (gravity) on surface of the earth, and the corresponding value predicted from a model of the gravitational field. If the attraction due to the effect of material between the plane of observation and the mean sea level known as the Bouguer correction (BC) is subtracted from the free-air anomaly, the corrected gravity field is called the Bouguer gravity anomaly denoted as g_{BGA} and is mathematically expressed in equation 11.0 as

$$g_{BGA} = g_{(obs)} + d_{gL} + d_{gFA} - d_{gB} - d_{gT} \quad 11.0$$

Where $g_{(obs)}$ represents the stations readings; d_{gL} represents the latitude correction; d_{gFA} represents the free-air correction; d_{gB} represents the Bouguer correction; and d_{gT} represents the terrain corrections. Inserting the numerical values into equation 11.0, the resultant value of the derived Bouguer gravity anomaly (g_{BGA}) is expressed and displayed in equation 12.0 as

$$g_{BGA} = g_{(obs)} - g_0 + 0.3086H - 0.0419rH - d_{gT} \quad 12.0$$

Drift correction

In the reduction of gravity data, the removal of drift due to effect of elastic creep in the spring of the field equipment is highly necessary (Ishola and Akinyemi, 2025). The instrumental drift of the gravimeter used in this survey was removed using a Geosoft computer algorithm routine application (Osazuwa,1988; Abubakar and Likkason, 2022). Theoretical assumption reveals a linear relationship between the observed drift and time as provided by the drift rate expressed in equation 13.0 as

$$\mu = \frac{(g_2 - g_1) - (Re_2 - Re_1)}{(t_2 - t_1)} \quad 13.0$$

Where g_1 and g_2 are absolute gravity values at the two end stations of a loop while Re_1 and Re_2 are tie observed reading (converted to milliGal) at times t_1 and t_2 respectively at those stations. If the sums station is reoccupied, then

$$g_2 - g_1 = 0 \quad 14.0$$

The repeated computation for loops continued until all observations are referred to an initial time, the drift correction for any intermediate station is thereby referred to the initial time t_0 Therefore, equation 13.0 becomes translated to equation 15.0.

$$\mu = \frac{(Re_2 - Re_1)}{(t_2 - t_1)} \quad 15.0$$

Judging by the assumption that drift of the instrument is a linear function of time over a short interval, it was ensured that all observations in a day were tied to the same time origin during a day's activity and the subsequent repeated observations at the same station after the drift correction was made to be equal to the former. Drift correction usually accompany each altimeter high value by applying free same cascade drift model.

EDITOR-IN-CHIEF
Prof. W. F. HILL [MALAWI]

The absolute elevation for each of the stations were determined for each altimeter using the height of the Bench Mark number specification to which they were tied. Due to the characteristic feature of the field equipment, the recorded field values front tie altimeters for each station were varying (Osazuwa, 1991). Therefore, the observed gravity value in mGals at the detailed station is expressed in equation 16.0 as

$$G_{obs} = g_1 - K\,[(Re_0 - Re_1) - \mu(t_0 - t_1)] \qquad 16.0$$

Where g_1 is the absolute gravity value at the first base station, K is the meter constant, Re_0 and Re_1 are the readings at the first base station and detailed station respectively while t_0 and t_1 are also the recorded times at the first base station and the detailed station respectively.

Based on field practices, since Gravity meter experiences drift over time due to temperature or mechanical instability; it means that, for instrumental drift to be corrected, repeated readings at base station should be undertaken at recorded times throughout the day. The reading is plotted against time and the drift is assume to be linear between consecutive base reading. Drift correction at time (t), is subtracted from the actual value. After drift correction, the difference in gravity between an observation point and base station is found by the multiplication of the differences in meter reading by the calibration factor of the gravity meter. With this information, we can compute the absolute gravity at the observation point from the known value of the gravity at the base station.

Gravity method is not only used in mineral exploration but have important application in the determination of tonnage of a previously located ore deposit; gravity method has been extensively used in the investigation of large and medium scale geological structure; gravity method has been used in the location of sedimentary basin where the interpreted structure has provided important constrain on theory of their mode of origin and the level of isostatic compensation of huge structure can be revealed by gravity methods; Gravity methods were once used widely to locate possible traps by hydrocarbon industries and can also be utilized in monitoring of volcanoes. In this study, mapping subsurface geological structures in which hydrocarbons are entrapped is another significant role gravity methods play (Khazari and Gabtni, 2018; Dilalos *et al.,* 2019). This is possible since the densities of different sedimentary rock formations are usually lower than those of the surrounding basement rocks. Therefore, the reconnaissance gravity survey provides useful information as to whether the sedimentary thickness beneath the earth's subsurface is sufficiently thick to justify further geophysical investigations. This present study represents a significant attempt at determining the depth to basement, structural types, delineating and identifying litho-geological characteristics for hydrocarbon and

EDITOR-IN-CHIEF
Prof. W. F. HILL [MALAWI]

solid minerals potentials using high-resolution airborne gravity data and interpretation in parts of Sokoto Basin, Northwestern Nigeria.

Data Acquisition and Processing

The airborne gravity datasets of the study area comprising of four (4) sheets (72,73, 95 and 96) were acquired by Nigerian Geological Survey Agency (NGSA) through Bureau Gravimetrique Internationale (BGI) France (Figure 6 and 7). The acquired datasets were analyzed and processed to produce the Bouguer anomaly map after being reprojected from the Universal Transverse Mercator of zone 32 Northing (UTM 32N) to that of (UTM 31N). The primary instrument is a high-resolution airborne gravity meter, such as the one developed by Fugro Airborne Surveys. Global Positioning System (GPS)/ Inertial Navigation System (INS) is used to accurately determine the position and orientation of the aircraft during the survey. Digital Recording System permits the data to be recorded digitally in formats like XYZ (X and Y for coordinates, Z for gravity measurements). The data in zipped format were first converted to text format and sorted out into the required longitudes and latitudes of the study area. The Microsoft excel tool and the Geosoft Oasis Montaj Version 8.4 geophysical software was employed for the processing, analysis including griddingof the data, and to interprete the gravity data (GOM, 2014). The raw aerogravity data obtained from the survey was reduced to separate their gravitational effects of subsurface density changes from those from other sources by employing necessary gravity corrections including free-air correction, bouguer correction and corrections for instrumental drift before they were imported into the software and converted into a dataset containing the longitude (X-channel), latitude (Y-channel), and Bouguer anomaly (Z-channel). The dataset imported into the Geosoft Oasis Montaj software was gridded using minimum curvature algorithm to generate the Bouguer gravity field which represents the observed anomaly of the entire investigated area. Depth is proportional to the slope of the line segment (Naidu, 1968, Spector and Grant, 1970; Layade *et al.,* 2021). This study requires a Regional-Residual Separation Techniques to ensure shallower signals. A high-pass filter was employed to obtain the residual anomaly map**.** Subsequently, residual anomaly map was produced from the bouguer gravity field by setting the cut-off wavenumber at 0.02 cycles/km to process the intermediate and shallow sources as the residual anomaly. The resulting residual anomaly was thereafter processed to produce the derivative of the field along the x-direction and the Analytic Signal map was generated to visualize the peak of anomalous sources and observed to be a bit noisy and hence, it was subjected to upward continuation; being upward continued at 1km in order to sharpen the edge of anomalous sources and geological boundaries. The accentuations of high frequency/low wavelength anomaly sources while attenuating short frequency/long wavelength anomaly sources, were also

EDITOR-IN-CHIEF
Prof. W. F. HILL [MALAWI]

achieved through a two-dimensional Fast Fourier transform (FFT2D) algorithm; Gaussian filter known as MIGMAP in Oasis Montaj Environment to filter off regional source structures linked with near surface causes; the regional-residual separation yielded the residual map (Graham *et al.,* 2014; Heshan and Heshan, 2016; Layade *et al.,* 2023). Regional residual separation was purposely carried out so as to remove the regional anomalies from the Bouguer gravity anomaly to obtain the residual anomalies. The residual component is due to relatively local near-surface masses while the regional component is that component of the total field arising from larger and deeper structures beneath the earth's surface. The regional-residual separation of the third order polynomial fitting provided the best visual fit for this work. The regional field g_R obtained from third polynomial represented by equation 17.0.

$$g_R = a_0 + a_1x + a_2x^2 + a_3x^3 + a_4x^4 + \dots a_nx^n \qquad 17.0$$

Where n is the order of the polynomial being used to approximate the regional fields. The coefficients are evaluated using the principles of least squares and the trends of different orders (*n*) are computed. The first vertical derivative filter was applied to the enhanced data to image the causative structures using equation 18.0 as applied in the Geosoft Oasis Montaj software.

$$\text{FVD} = -\frac{\delta A}{\delta Z} \qquad 18.0$$

Forward and inverse modelling techniques were used to obtain the numerical estimates of the depth and dimension of the sources of anomalies based on Euler equations (Biswas *et al.,* 2017). This was practically achieved with the utilization of potent Q-3D tool of the Geosoft Oasis Montaj software with selected regions based on the contour cluster configuration beneficial for modelling (Obiora *et al.,* 2016; Onyeche *et al.,* 2023; Ishola and Akinyemi, 2025). The standard 3D Euler-deconvolution method is based on homogeneity equations that relate the gradients components of the potential filed to the source location. The structural index (SI), having values ranging from 0-2 for gravity sources (Hesham and Hesham, 2016; Tompson, 1982). These sources are described by different theoretical geometries with corresponding S1 as follows; sphere-(SI=2), vertical line end (pipe)- (SI=1), Horizontal line (cylinder)-(SI=0) respectively (Reid *et al.,* 2014). These sources are described by different theoretical geometries with corresponding SI as follows; sphere-(SI=3), vertical line end (pipe)-(SI=1), Horizontal line (cylinder)-(SI=1) and thin sheet edge-(SI=0) respectively (Reid *et al*., 2014; Ibim *et al.,* 2025) is defined as; the coordinate of the measuring point are x, y, and z; b is a base level; the coordinate of the source location is $x_\circ$, $y_\circ$, and $z_\circ$; while T is total potential field respectively. A square widow

EDITOR-IN-CHIEF
Prof. W. F. HILL [MALAWI]

of considerable size of 3000m by 3000m containing number of grid cells in the gridded database was used in order to accommodate the depth of sources, as investigated by past investigations in the study area. In computing the standard Euler deconvolution solutions, the recommendations from the findings of (Reid *et al*., 2014) were adopted by using the different structural indices of 0, 1 and 2 were tried in solving the solutions but only SI equals 0 gave a geologically meaningful solutions which reveals that the area is possibly characterized by structures like faults, contacts and thin sheet edge (dike), (Reid *et al.,* 2014).

Qualitative Analysis

Qualitative Analysis of gravity data involves visually examining and interpreting gravity maps to identify patterns, anomalies, and structural trends related to subsurface geology. This approach focuses on identifying features like lineaments (linear anomalies) which can indicate faults contacts, and other tectonic features. It is a complementary approach to quantitative method helping to develop a broader understanding of the subsurface. Visual Inspection and Pattern Recognition: Identifying lineaments: Linear anomalies on gravity maps can suggest the presence of faults, contacts or other linear structural features and recognizing circular or oval anomalies: Examining the overall pattern of gravity anomalies can help in understanding the regional geological settling and tectonic history. Interpreting Gravity Anomalies in a Geological context involves relating observed anomalies to known Geology while the qualitative analyses involve relating gravity anomalies to existing geological maps and data, helping to refine understanding of the subsurface. Considering Density Contracts where Gravity anomalies are caused by density variations within the subsurface, so understanding the likely density distributions of different rock type is crucial; Analyzing Filtering Techniques where various filtering techniques are applied like low-pits on high pass filters can enhance specific features or isolate different scales of anomalies; using Derivative Maps where the Derivative maps (like the total horizontal derivative) can highlight dares with high gravity gradients which often correspond to faults or contacts. The Complementariness to quantitative methods are namely, Providing Initial Insights as qualitative analysis can provide a starting point for more detailed quantitative modelling and inversion techniques; Guiding Model Development such that the initial qualitative interpretations can inform the development of subsurface models and the selection of appropriate model parameters; and the Interpreting Inversion Results: Qualitative analysis can help in interpreting the results of gravity inversion, ensuring that the models are geologically plausible and consistent with other data.

In essence, qualitative analysis of gravity data is a crucial step in understanding the subsurface providing a visual and interpretative framework for identifying a visual and

EDITOR-IN-CHIEF
Prof. W. F. HILL [MALAWI]

interpretative framework for identifying key geological features and guiding further investigations. Qualitative interpretation of gravity anomalies may be accomplished by analogy to mathematical experimental survey over known structures (Marttinez-Moreno *et al*., 2015). In some instance it may be considered as diagnostic. For example, a gravity low located on a favorable geological province may be indicative of the province of sand dome. In the qualitative interpretation of gravity and magnetic maps, geophysicists are usually interested in linear anomalies (Lineaments) as indicators of subsurface faults, contacts and other tectonic features (Strykowski, 2017; Ishola and Akinyemi, 2025).

Generation and Interpretation of Bouguer Anomaly Map

Gravity data are collected using gravimeters either terrestrially, on marine vessels, or via airborne surveys. Accurate positioning is obtained through GPS systems. Raw gravity data are corrected for various effects: Latitude Correction accounts for the variation of gravity with latitude, the Free-Air Correction removes the effect of elevation above sea level. Bouguer Correction adjusts for the gravitational attraction of the rock mass between the measurement point and sea level, the Terrain Correction accounts for nearby topographical variations. Reduction to Bouguer Anomaly uses the corrected gravity values are used to compute the Bouguer anomaly, which reflects subsurface density variations. Mapping enables the utilization of Bouguer anomaly values are interpolated and contoured to produce a map, typically using software like Oasis Montag, Surfer, or GMT. In the interpretation of Bouguer Anomaly Map, the High Bouguer Anomalies are Indication of regions of higher density materials such as igneous intrusions or mafic rocks while the Low Bouguer Anomalies: Suggest areas of lower density, often associated with sedimentary basins or crustal thinning.

Generation and Interpretation of First Vertical Derivative Map

The First Vertical Derivative (FVD) is a mathematical operation applied to gravity data that measures the rate of change of the field with respect to vertical distance ($\delta F/\delta z$). It enhances the high-frequency components of the anomaly, making it easier to locate shallow geological structures and edges. The Pre-processing and Corrections enable the raw data to be corrected for drift, diurnal effects, terrain, latitude (for gravity), and other influences. The FVD is typically computed in the frequency domain using Fast Fourier Transform (FFT) by multiplying the Fourier transform of the data by a factor proportional to the wavenumber. The derived FVD values are gridded and plotted as contour or color maps. Peaks and zero-crossings in these maps indicate the positions of geological boundaries and contacts. On the interpretation of First Vertical Derivative (FVD) Maps, Edge Detection and Structural Mapping reveals that FVD maps sharpen anomaly boundaries, making it easier to delineate faults, dikes, lithological contacts, and intrusive

EDITOR-IN-CHIEF
Prof. W. F. HILL [MALAWI]

bodies while the Enhancing Shallow Features reveals that The FVD amplifies high-frequency, shallow-source anomalies, helping to distinguish them from deeper sources.

Generation and Interpretation of First Horizontal Derivative Maps

The First Horizontal Derivative (FHD) map enhances the rate of change of a gravity field in the horizontal (x and y) directions. It highlights lateral contrasts in subsurface physical properties, often associated with geological boundaries like faults, contacts, or dykes. The steps in Generation involves the Pre-processing and Corrections where aw data undergo corrections for diurnal variations, instrumental drift, topography, latitude, and other factors. The Calculation of Horizontal Derivatives where the first horizontal derivatives (δF/δx and δF/δy) are computed either: In the frequency domain (using Fast Fourier Transform [FFT] techniques); In the space domain (using finite-difference approximations). This operation emphasizes the lateral gradients, marking sharp changes in subsurface density or magnetization. Gridding and Mapping enables the derived horizontal derivative values to be interpolated into a grid and displayed as color or contour maps. The interpretation of First Horizontal Derivative (FHD) Maps involves Anomaly Shape Analysis where the shape, width, and amplitude of horizontal derivative anomalies can give clues about the nature, size, and depth of subsurface features and Structural Trends Identification where the FHD maps reveal the orientation and continuity of subsurface structures, which may not be evident in total field or Bouguer anomaly maps.

Analytical Signal Map

The Analytical Signal (AS)is a mathematical combination of the horizontal and vertical derivatives of gravity or magnetic field data. It's used to locate and outline the edges of subsurface bodies such as faults, contacts, or intrusive rocks by emphasizing zones of maximum gradient, which typically occur over the edges of causative structures. Using mathematical expression for 2D or 3D in equation 1.0, the total amplitude of the analytical signal is calculated as x in equation 19.0.

$$\text{AS (x, y)} = \left(\frac{\delta F}{\delta x}\right)^2 + \left(\frac{\delta F}{\delta y}\right)^2 + \left(\frac{\delta F}{\delta z}\right)^2 \qquad 19.0$$

According to Nabighian, 1972a, the analytical signal, AS_1 (x, z) is defined as in equation 20.0

$$AS_1\ (\text{x, z}) = \frac{\delta \varphi_{(x,z)}}{\delta x} - j\ \frac{\delta \varphi_{(x,z)}}{\delta z} \qquad 20.0$$

EDITOR-IN-CHIEF
Prof. W. F. HILL [MALAWI]

Where $\varphi_{(x,z)}$ represents the magnitude of the anomalous total gravity field, j is the imaginary number, and x and z are cartesian coordinates for the horizontal and vertical directions respectively. The horizontal and vertical derivatives which comprises the real and imaginary parts of the 2D analytical signal are related by equation 21.0

$$\frac{\delta\varphi_{(x,z)}}{\delta x} \leftrightarrow j\ \frac{\delta\varphi_{(x,z)}}{\delta z} \qquad 21.0$$

Where $\leftrightarrow$ in equation 21.0 is denoted as a Hilbert transformation while the local wave number is displayed in equation 22.0 as

$$C_1 = \frac{\delta}{\delta x} tan^{-1}\left[\frac{\frac{\delta\varphi}{\delta z}}{\frac{\delta\varphi}{\delta x}}\right] \qquad 22.0$$

(Nabighian, 1972a; Nabighian, 1972b; Layade *et al.*, 2023)

Therefore, the analytic signal could be defined as a second order derivative AS_2 (x, z) as expressed in equation 23.0

$$AS_1\ (\mathrm{x, z}) = \frac{\delta^2\varphi_{(x,z)}}{\delta x} - j\ \frac{\delta^2\varphi_{(x,z)}}{\delta z} \qquad 23.0$$

Equation 5.0 will further give rise to the second wave number C_2 defined in equation 24.0 as

$$C_2 = \frac{\delta}{\delta x} tan^{-1}\left[\frac{\frac{\delta^2\varphi}{\delta z^2}}{\frac{\delta^2\varphi}{\delta z\delta x}}\right] \qquad 24.0$$

After the acquisition and preprocessing of the raw gravity data, first derivatives in the x, y, and z directions are computed (usually using filters in Geosoft Oasis Montaj, or other GIS/geophysical software). The analytical signal formulae are applied, the result of the analytical signal map is displayed as a contour or color-shaded map, where high values are indications of the location of source edges while low values are indications of background regions. The interpretation of Analytical Signal Maps reveals High-Amplitude Zones to depicts edges of density or susceptibility contrasts like faults, lithological contacts, or intrusive bodies while consequent Shape and Distribution assist in inferring the geometry, trend, and extent of subsurface structures.

EDITOR-IN-CHIEF
Prof. W. F. HILL [MALAWI]

Residual Anomaly Map

A residual anomaly map is a tool used in gravity survey, to identify subsurface structures or features by isolating anomalies from the regional trend. They are generated by collecting gravity data over the area of interest by applying techniques like filtering, wavelet analysis to separate regional and residual anomalies. The residual anomalies are calculated by subtracting the regional trend from the observed data. In Anomaly Identification, areas with significant residual anomalies, which may indicate subsurface features or structures are identified. Geological Significance is achieved by Interpreting the anomalies in the context of the local geology while considering factors like lithology, structure, and tectonic history.

Regional Anomaly Map

A regional anomaly map is a tool used to identify large-scale subsurface features or structures. Data is collected from gravity data over area of interest and techniques such as filtering, smoothing, or upward continuation are used to emphasize regional trends. The regional anomaly is calculated by fitting a polynomial or spline surface to the data. The regional anomaly map involves trend analysis where the regional trends and patterns in the anomaly map are identified and the geological significance is consequently achieved by Interpreting the regional anomalies in the context of local geology.

Quantitative Analysis

This approach involves making numerical estimates of certain magnetic signatures that yielded likely geological features and their depth sources (Reeves, 2005; Ishola and Akinyemi, 2025).

Generation and Interpretation of Euler Deconvolution

Euler Deconvolution is an automatic interpretation technique used in gravity and magnetic data analysis to estimate the location (x, y), The depth (z) of potential field sources (like faults, dykes, contacts, and intrusive bodies). It's based on the Euler homogeneity equation, which relates the spatial derivatives of the measured field to the location of its causative source. The 3D Euler deconvolution method was used for the estimation of the depth to the basement of anomalous density present in the study area. The basic Euler's homogeneity equation which connects the potential field and its gradient components to the source location and can be interpreted as a structural index (SI) which serves as the foundation for the standard 3D Euler deconvolution method (Thompson, 1982; Layade *et al.,* 2023). For a source of a given geometry, the SI is assumed to be an exponential factor that represents the rate at which the potential field decays

EDITOR-IN-CHIEF
Prof. W. F. HILL [MALAWI]

with distance. The standard Euler 3D form of Euler's equation is expressed in equation 25.0 as

$$(x_i - x_0)\frac{\delta F}{\delta x} + (y_i - y_0)\frac{\delta F}{\delta y} + (z_i - z_0)\frac{\delta F}{\delta z} = \eta(\mathrm{B} - P_i) \qquad 25.0$$

The measuring point's coordinates of source (x, y, and z$_\circ$); x_0, y_0 and z_0 are the coordinates of thew source location, whose total field is detected at x, y, and z; B represents the base level; SI is the structural index (SI) and P_i is the total potential field. The SI which corresponds to different source geometry as proposed by Reid *et al.,* 1990 for potential field measurements. The data collected was tested for different source geometries i.e., fault, horizontal, cylinders and spheres which corresponds to the structural indices 0, 1, and 2 respectively. The generation and interpretation of Euler Deconvolution Solutions follows thus as the gravity data is corrected and enhanced (often with derivatives) in data preparation. A uniform grid is created. The selection of Structural Index (N) reflects the type of geological structure where 0 stands for contacts, 0.5 for faults, 1 for thin dykes or pipes, 2 for cylindrical bodies, 3 for spheres while the numerical solutions of Euler's Equation are computed for sliding windows across the data grid and gives the estimated positions and depths of potential field sources. Depth estimates from clustered solutions indicate the likely depth of causative sources (Ishola *et al.,* 2025; Sfada, 2025). The source type and geometry are used in comparing solutions obtained using different structural indices helps infer the type of source (fault, dyke, sphere, etc.) while th structural mapping is consequently used for the lateral distribution of Euler solutions highlights linear or point-source features, correlating them with faults, lineaments, or intrusions.

Analytical Mapping and Positioning Tools

The data acquired from NGSA was prepared with Microsoft Excel, processed using Oasis Montaj 8.4v, the data was imported and transferred to UTM Zone 31N from UTM Zone 32N to maintain a constant coordinate system and avoid misinterpretation of data by minimizing distortion over certain areas in the study location as it belongs to UTM Zone 31N (Figure 8). According to Nigeria Geological Survey Agency (NGSA, 2017), the acquired data set was part processed by Bureau Gravimetrique Internationale (BGI), France. using Universal Transverse Mercator of Zone 32N (UTM-32N) projection and World Geodate System, 1984 (WGS84) as the reference datum. The WGS84 is a global datum used for determining position on the earth's surface (Ishola and Akinyemi, 2025). The WGSS84 is a reference system used by the satellite navigation system like GPS and is used by the satellite navigation systems like GPS and is used in various mapping applications. It is used for determining positions on the earth's surface. It is a standard reference system used

by satellite Navigation systems like GPS and is also used in various mapping applications. The WGSS84 datum is defined and maintained by the United States National Geospatial-Intelligence Agency (NGA). Coordinates computed from GPS received are typically provided in terms of the WGS84 datum. WGS84 is compatible with the International Terrestrial Reference System (ITRS). De-culturing, tie-line and micro-levelling are some of the pre-processing operations carried out on the data (Ishola and Akinyemi, 2025). The dataset was given out by NGSA as an ASCII file comprising of X, Y and Z columns corresponding to the longitudes, latitudes and their matching total gravitational field contracts respectively (Hakney and Featherstone, 2003; NGSA, 2005; Gilardoni *et al.*, 2016).

The data set was invaded in Oasis Montag Software database to obtain the raw total gravitational field contracts (Z-total). The raw dataset was then re-projected to Universal Mercator of zone 31N (UTM-31N) in order to minimize distortions due to the curvature of the earth and to have relationship with the subsurface geology for easier interpretations (Pavlis *et al.,* 2007; Barthelmes *et al.,* 2016;). This was necessary because the study location fall within UTM-31N (Figure 8).

World Geodetic System 1984 (WGS,1984)

The WGS84 is a 3-dimensional coordinate reference frame for establishing latitude, longitude and heights for navigation, positioning and targeting for the DOD, IC, NATO, International hydrographic office and the International Civil Aviation Organization. WGS84 represents the best global geodetic reference system for the earth available at this time for practical applications of mapping, charting, geo-positioning and navigation (WGS, 1984). This standard includes the definition of the coordinate systems fundamental and derived constants, the ellipsoidal(normal), Earth gravitational model (EGM), a description of the associated World Magnetic Model (WMM) and the current list of local datum transformations, NGA and the National System for Geospatial Intelligence (NSG), DOD IT Standards Registry (DISR). Figure 8 represents Universal Transverse Mercator (UTM) grid zone of the world where the study area was referenced. The document UTM Grid Zones of the world was compiled by Alan Morton in 2015 but the official UTM system was developed by the United States Army Corps of Engineers in the 1940s. Morton's guide has since been a popular, independent representation of the 60-zone longitudinal and 20-band latitudinal system. There are 60 longitudinal projection zones numbered 1 to 60 starting at 180°W (Ishola and Akinyemi, 2025). Each of these zones is 6 degrees wide, apart from a few exceptions around Norway and Svabard. There are 20 latitudinal zones spanning the latitudes 80°S to 84°N and denoted by letters C to X omitting the letters I and O. Each of these is 8 degrees south-North, apart from zone X which is 12 degrees south-north. The study area was referenced by quoting the longitudinal zone number,

EDITOR-IN-CHIEF
Prof. W. F. HILL [MALAWI]

followed by the latitudinal zone letter; as 32N from that of 31N after reprojection, just as the southern end of South America gives 19F. within each longitudinal zone represents the transverse Mercator projection that is used to co-ordinates (eastings and northings) in metres. For the eastings, the origin is defined as a point 500,000m west of the central meridian of each longitudinal zone, giving an easting of 500,000m at the central meridian. For the northings in the northern hemisphere, the origin is defined as a point 10,000,000m south of the equator. The co-ordinates thus derived define a location within a UTM projection zone either north or south of the equator, but because the same co-ordinate system is repeated for each zone and hemisphere, it is necessary to additionally state the UTM longitudinal zone and either the hemisphere or latitudinal zone to define the location uniquely worldwide (Morton, 2015; Sylvester *et al.,* 2018; Ishola and Akinyemi, 2025).

Earth Gravitational Model

This division in the office of Geomatics at NGA is responsible for collecting, processing and evaluating gravity data (free-air and Bouger gravity anomalies). These data are then used as gravimetric quantities such as mean gravity anomalies, geoid heights, deflections of the vertical and gravity disturbances (WGS, 1984). These quantities are used in World Geodetic System, 1984 support, navigation systems, mapping projects and different surveys. An Earth Gravitational Model (EGM) is a set of geopotential coefficients used in a spherical harmonic expansion to create a global potential surface to coincide with mean sea level (M.S.L). This surface is called a geoid and it fluctuates above and below the reference ellipsoid surface established by WGS84 (Ishola and Akinyemi, 2025). The relationship between EGM and WGS forms the foundation of modern geodesy, navigation, and geophysics. The WGS84 provides a geometric provides a geometric framework (ellipsoid) to define horizontal positions, while the EGM (such as EGM2008) provides a physical model (geoid) to define heights and vertical datum. Their combined use allows for precise 3D positioning and gravity-related studies. WGS84 serves as a geometric framework that defines the mathematical earth as a geocentric, earth-fixed ellipsoid. It is the standard reference frame used by GPS for latitude, longitude, and ellipsoidal height (*h*). EGM serves a physical model that defines the physical earth (geoid) representing mean sea level (MSL) and an equipotential surface of the earth's gravity field. It identifies anomalies and undulations where gravity differs from a smooth ellipsoid. EGM allows the conversion of ellipsoid heights (h from GPS) to orthometric heights H-height above the mean sea level using the equation (h = H+N); N stands as the geoid undulation. EGM and WGS84 relationship have significant impacts on location and position in Absolute accuracy as the integration of WGS84 with EGM (EGM96 or EGM2008) allows GPS to provide 3D coordinates worldwide. Current refinements allow

EDITOR-IN-CHIEF
Prof. W. F. HILL [MALAWI]

alignment with the latest International Terrestrial Frame (ITRF) within a few centimeters improving navigation and survey accuracy; height precision is another significant factor where EGM models are crucial for mapping true elevations, as GNSS only provides ellipsoidal heights which do not reflect water flow or true vertical; the relationship provides dynamic data since WGS84 is a dynamic datum and it accounts for tectonic plate motions over time, keeping locations accurate despite shift (Karpic *et al.,* 2016). The integration has overwhelming impacts on mining and exploration, subsea positioning, construction and civil engineering and tectonic monitoring. Therefore, WGS serves as the mathematical base map while EGM acts as the physical topography map of the earth. Together, they offer a consistent 3D framework for global and local navigation, mapping and exploration (Smith *et al.,* 2018; Yilmaz *et al.,* 2018).

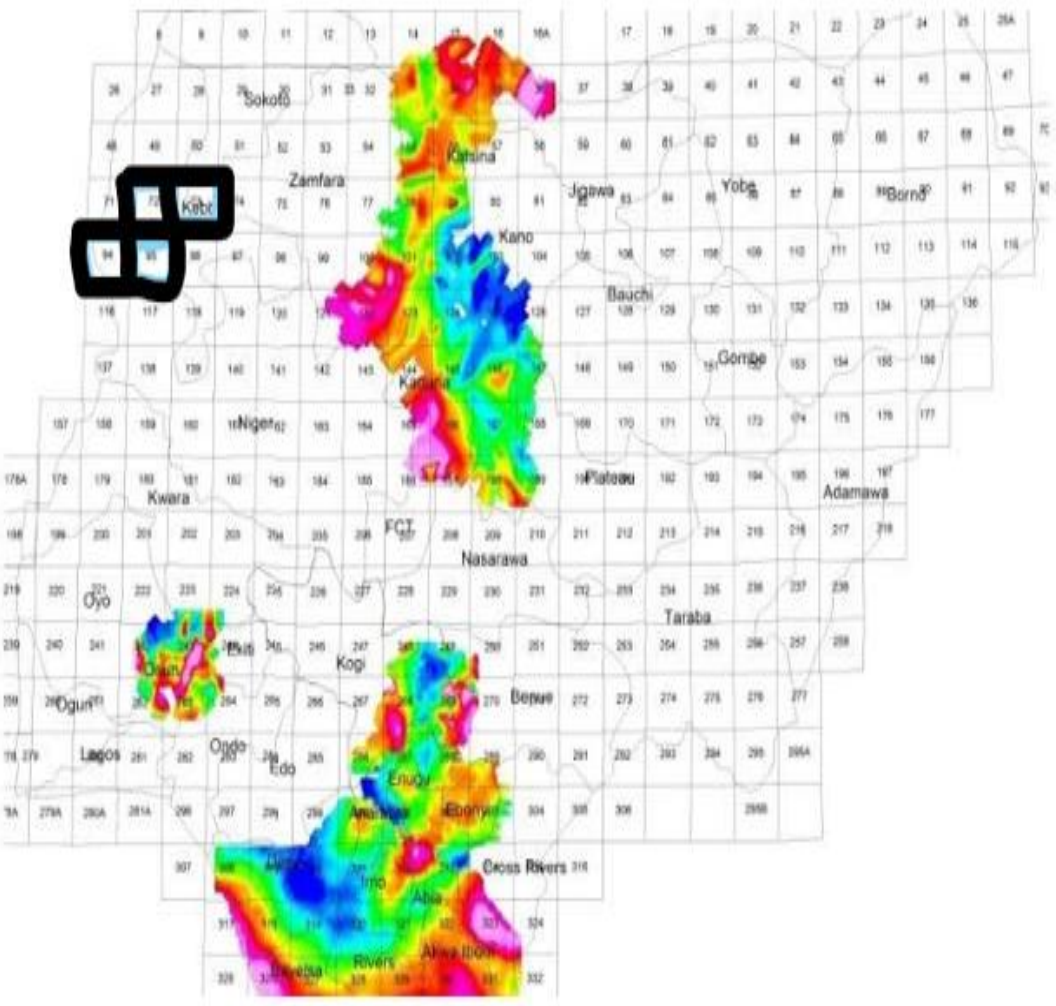


Figure 6: Map of Nigeria showing the sheet numbers of the study area and other associated sheets (NGSA, 2017)

EDITOR-IN-CHIEF
Prof. W. F. HILL [MALAWI]

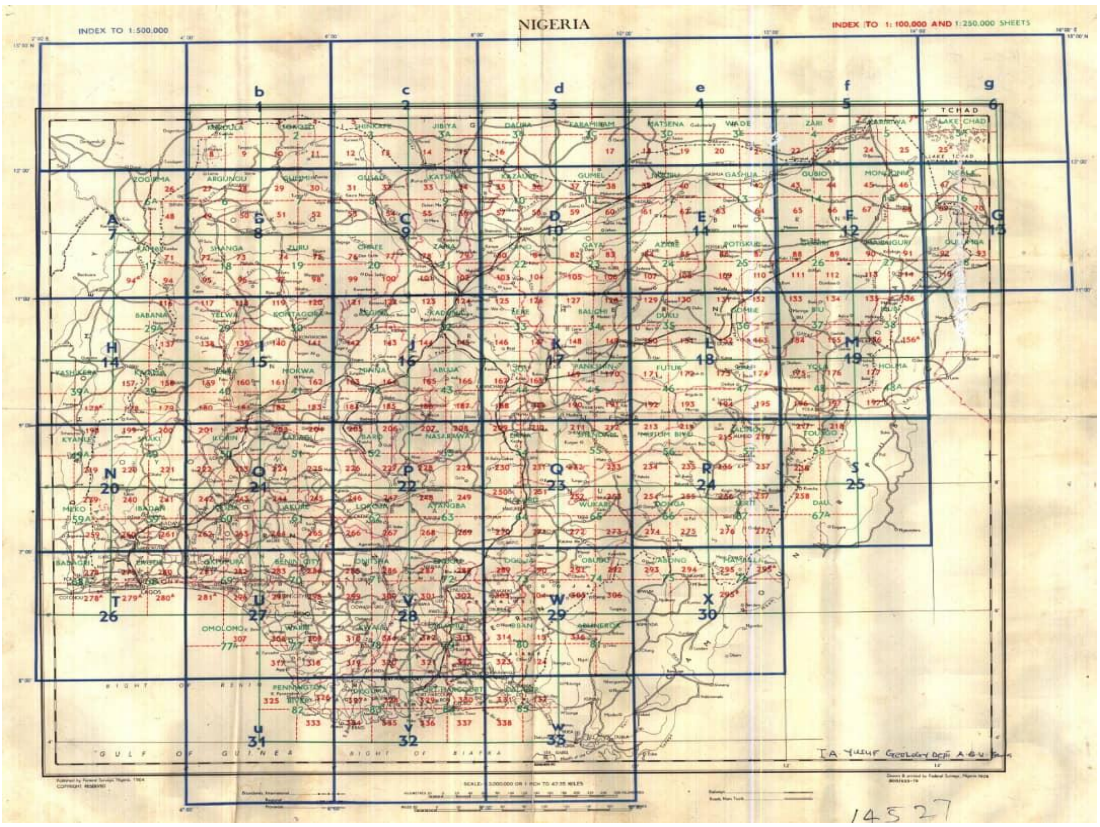


Figure 7: Map of Nigeria showing different towns and their index distribution (NGSA, 2006)

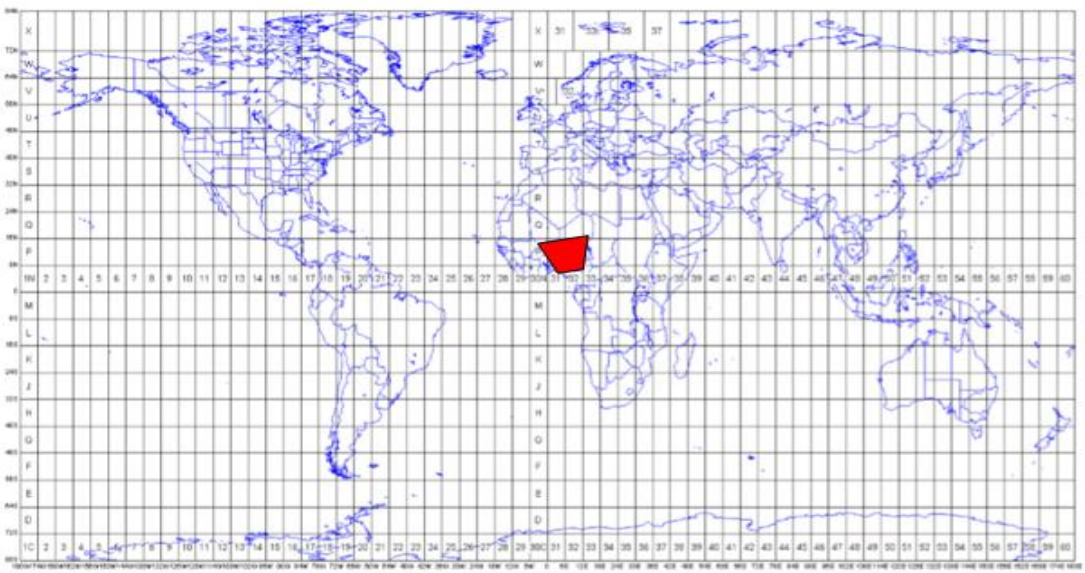


Figure 8: Map of the World showing UTM Grid zone for Nigeria and other geographical location of the World (Morton, 2015; modified by Ishola and Akinyemi, 2025)

EDITOR-IN-CHIEF
Prof. W. F. HILL [MALAWI]

Bouguer Gravity Anomaly Map

The Bouguer Gravity Anomaly Map is presented in Figure 9**.** The range of gravity values observed on the total field ranged from -71.67 to -28.20 mgal. Region of relatively high-density anomaly (Red and Pink regions) can be observed in the North around Zokwa, Madiji and Aida and the South-West direction comprising of Kashe Hill, Farin Ruwa, Lafagu, Tunga Numaruwa extending to the extreme SE of the study area. Also, regions of intermediate gravity anomalies (represented by yellow and green region) like Rorukos Hill and partly Beri while regions of typically low gravity anomalies (represented by the deep blue region) encompassing Kwaifa and Koko/Bese at the central part of the study area. The observed region of low-density anomaly map may represent causative bodies for hydrocarbons and solid mineral entrapments with deep burial area ranging from (54.24l to 48.12 mgal) in the North-West direction to the South-East (Figure 9). The gravity anomaly map revealing variations of low to high gravimetric values is an indication of high conformity to the lithological differences in the sub-surface. The observed varying high, intermediate and low anomalies in NW to SE and E-W trends are resultant effect of fold patterns in the South-eastern part of the lullemmenden basin (Sokoto basin in particular). These alternated anomalies are primarily due to the density contrast between the sedimentary blanket and some portion of crystalline basement in Taloka Formation. The high gravity in part of Sokoto basin is significant characteristics feature.

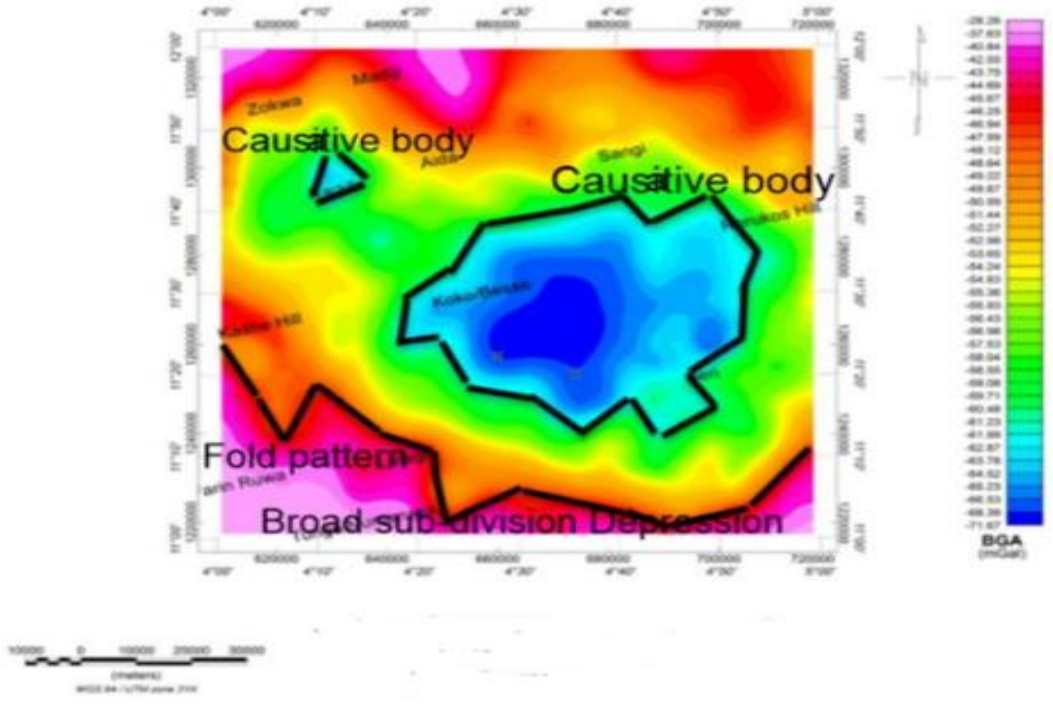


Figure 9: Bouguer Gravity Map of the study area.

EDITOR-IN-CHIEF
Prof. W. F. HILL [MALAWI]

Bouguer map with a strong positive oval shape anomaly (> -28.26mgal) having SE trend. The structural trend pattern from the map trending in the S-E direction is associated with deep basinal area of the causative body (anomalous zone) determined from the gravity survey were found to range from (-54.24mgal) in the West corner of fold patterns and (-48.12mgal) in the North-West to South East part. The Bouguer gravity anomalous zone displayed negative values while the deep basinal area of the causative body fall within Gwandu, Kalabaina, Dange, Gamba, Wurno and Taloka formation which are representatives of two different but complementary events; an older-events of most probably of continental intercalaire and pre-cretaceous episodes that induced major folding and faulting trending NE-SW and ENE respectively.

Fault Structure in Parts of Sokoto Basin

Figure 10 represent the fault structures superimposed on the Bouguer Anomaly map of the study area. This confirms the presence of lineaments like faults and other intrusive contacts like dike and/or sill in the study area.

Regional- Residual Gravity Separation

In this study, a purely analytical method was used with (Geosoft Oasis Montaj 8.4v) in which matching of the regional by a polynomial surface of low order exposes the residual features as random errors. A first order polynomial surface was considered adequate for estimating the regional effect. Regional- residual separations process was applied to gravity dataset in order to estimate the amplitude of the regional background. Upward continuation was used to separate a regional gravity anomaly resulting from deep sources from the observed gravity (Figure 9).

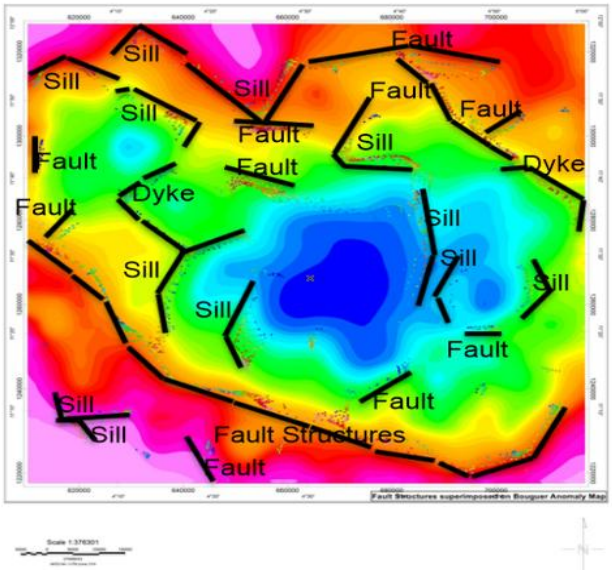


Figure 10: Fault Structures superimposed on Bouguer Anomaly Map of the study area.

Regional Anomaly Map of Parts of Sokoto Basin

The regional field of (Figure 11) is a plane dipping gently in a NE-SW direction. The regional effect corresponds to low frequencies therefore the anomalies are usually of long wavelength displaying a gradual change in values while the

EDITOR-IN-CHIEF
Prof. W. F. HILL [MALAWI]

residual anomalies which are due to local effects may show large variations (Blakely, 1995; Blakely, 1996; Abubakar and Likkason, 2022). There are several methods of removing the unwanted regional, some approach is entirely graphical while others are analytical. In some area, the graphical methods are incorporated in the analytical methods. In the study area, the regional gravity values entirely exhibited negative and were found to range from a maximum of -52.37mgal to a minimum of -54.98mgal (Figure 11). The highest regional gravity is exhibited around Tunga Numaruwa followed by Farin Ruwa and Lafagu while the lowest is exhibited by Madiji alongside Zokwa.

Residual Map of Parts of Sokoto Basin

The Bouguer Gravity Field contains anomalies that are near surface and those due to regional sources. Before any meaningful interpretation of the data can be carried out, it is highly significant to filter off regional anomaly sources from the field to accentuate shallow anomalous sources. This was accomplished by generating the Radially Averaged Power Spectrum (RAPS). The generated RAPS in (Figure 12) can then be utilized for the visualization of both deep-seated and shallow potential field sources while the possible noise levels associated with them are visualized alongside. Regional anomaly sources with frequency of about 0.3 cycles/km were observed and were consequently filtered off using a Gaussian filter. This filter accentuates shallow anomaly features while attenuating regional sources that are

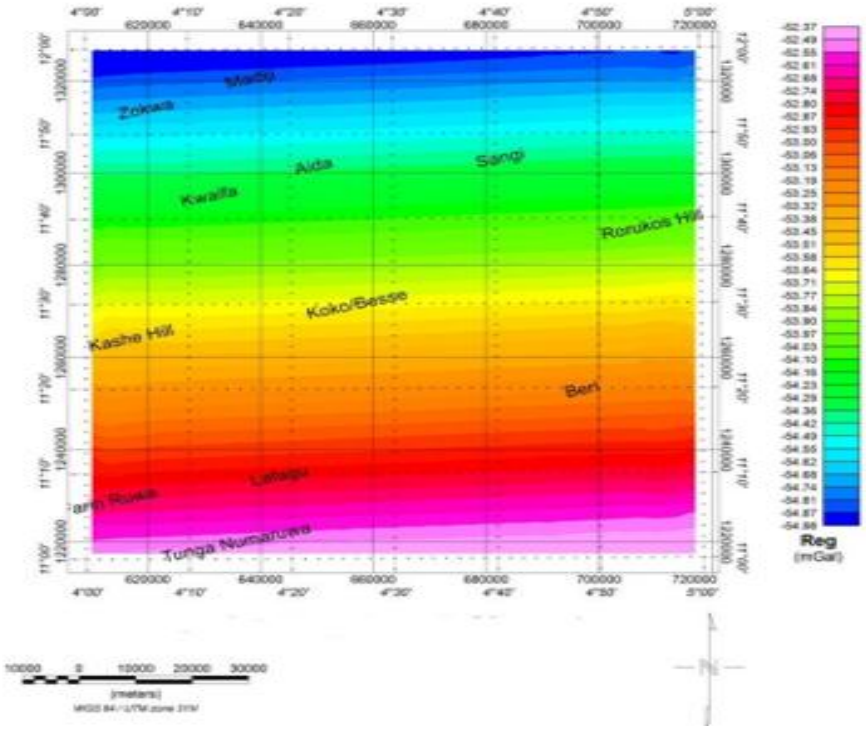


Figure 11: Regional Map of Parts of the study area.

EDITOR-IN-CHIEF
Prof. W. F. HILL [MALAWI]

otherwise referred to as noise in this work.

The residual anomaly at any point is then calculated as the difference between the observed Bouguer anomaly $g_{(obs)}$ and the regional effect of g_R at that point; this is mathematically expressed in equation 26.0 as

$$g_{BGA} = g_{(obs)} - g_R \qquad 26.0$$

The residual anomalies at all the points were gridded and contoured through the application of (Geosoft Oasis Montaj Version 8.4v**). (**Figure 12) is the resulting residual anomaly map for the separated Bouguer Anomaly grid which displayed the gravitational effect of the near surface and local geologic structures in the study area. The Gaussian filtered anomaly which has values found to range from -18.20mgal (minima) to 24.21mgal (maxima), accentuated shallow anomalies that were partly obscured by regional sources as observed by some deep blue patches made more visible in the southern part of the area around Beri. The blue regions corresponding to regions of low gravity anomaly are likely area with fault lines or dikes which would be suitable entrapments for hydrocarbons and solid minerals in the near subsurface. Also, the larger features generally show up trends which continue or run smoothly over considerable very large areas, and they are caused by deeper heterogeneity of the earth's crust superimposed on these trends but frequently camouflaged by them lies smaller, local disturbances which are secondary in terms of size but primary in structural significance (Abubakar and Likkason, 2022). These are the residual anomalies which may provide the direct evidence for reservoir type structure or mineral bodies. These were not much observed difference in density contrasts both at residualization and total gravity **(**Figure 12).

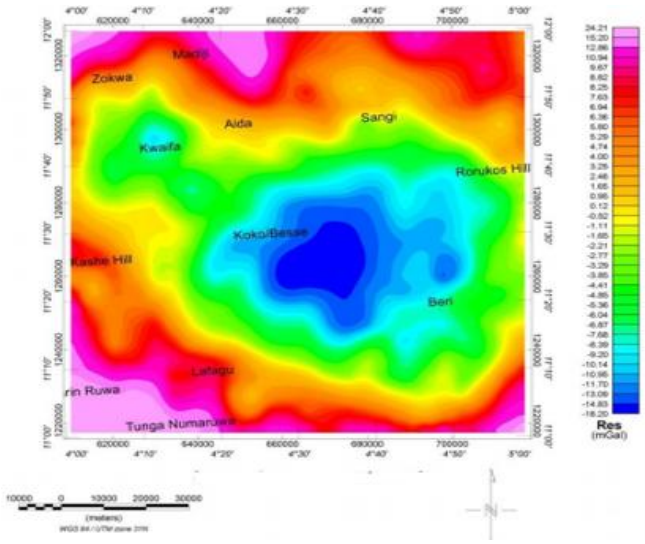


Figure 12: Residual Anomaly Map of the study area

Analytic Signal and Gravity Anomalies

Analytic Signal is a mathematical transformation of gravity data that is used to enhance the identification of subsurface structures and their boundaries. It essentially amplifies the gradients in the gravity field, making it easier to pinpoint locations of contacts between different geological units

EDITOR-IN-CHIEF
Prof. W. F. HILL [MALAWI]

while gravity anomalies represent deviations from the expelled gravity field based on the earth's rotation and density distribution. Low gravity anomalies usually indicate areas with less dense materials or voids while high gravity anomalies (positive anomalies) suggest denser materials or sub surface structures, they provide different perspectives. Analytic signal focuses in identifying edges and boundaries while gravity anomalies highlight regions with varying density contracts. Imagining the subsurface fault identified in the study area; the analytic signal would likely show a high amplitude signal along the fault line indicating its boundary. The gravity anomaly, on the other hand, might show a low-gravity area associated with the fault, potentially indicating a zone of weaker or less dense rock. Therefore, locations of low gravity generally do not correspond to locations of high or low analytic signal. Analytic signal is only a derived quantity from gravity data used to identify contacts and edges of geological structures while low gravity typically indicates areas with lower density contracts. For instance, through Kwaifa, Koko/Besse have low gravity but possessed higher analytic signal while Tunga Numaruwa and Farin Ruwa had both higher gravity and higher Analytic signal compared Lafagu, Aida, Berri with low Bouguer gravity value but higher Analytic signal (Figure 9 and Figure 13**).**

Analytic Signal Map

The analytic Signal Map displayed in Figure 13 reveals amplitude signal that varied from 0.0003 to 0.00107mgal/m higher analytic signal occurred most significantly as patches dominating the South and North-West of the study area with lower analytic signal also occurring in patches across the study area. Higher range of analytic signal ranging from 0.04mgal/m to 0.1mgal/m have been reported in Agbabu bituminous deposits of Dahomey Basin southwest Nigeria (Layade *et al.,* 2023). Also, higher range of analytic signal value ranging from 0.002mgal/m to 0.02mgal/m with high gravity responses spatially distributed in Abeokuta (Layade *et al.,* 2021). The area with comparably high analytic signal (denoted by red and pink region) corresponds to area with high density contrasts or peaks of gravity anomaly while regions with low analytic signal does not exclusively or necessarily indicate low density contrasts. The analytic signal is primarily influenced by the vector component of the model, not just the density contrast itself while it can be used to estimate depth, the signals shape and amplitude depend on the sources of gravity and depth regardless of the ambient gravity field or gravity direction. Low analytic signal amplitude might be associated with shallow sources or even those with low gravitation rather than exclusively with low density contrasts. The amplitude of the analytic signal is influenced by the vector component of the gravity source not just the density contrast. This means the strength and orientation of the source's gravitation play a significant role in determining the signals magnitude. The analytic signals shape is primarily determined by the depth of the source. A low analytic signal would indicate a shallow source or a

EDITOR-IN-CHIEF
Prof. W. F. HILL [MALAWI]

source of low gravitation, even if the underlying density contrast is relatively high. Therefore, though the analytic signal can be used to identify areas of potential interests, it does not translate to low density contrasts. Low signal amplitude can be caused by several factors including shallow sources, low gravitation or even certain types of geological structures. To understand gravity data and density variation. It is crucial to consider the entire context of the geological setting and the properties of the sources.

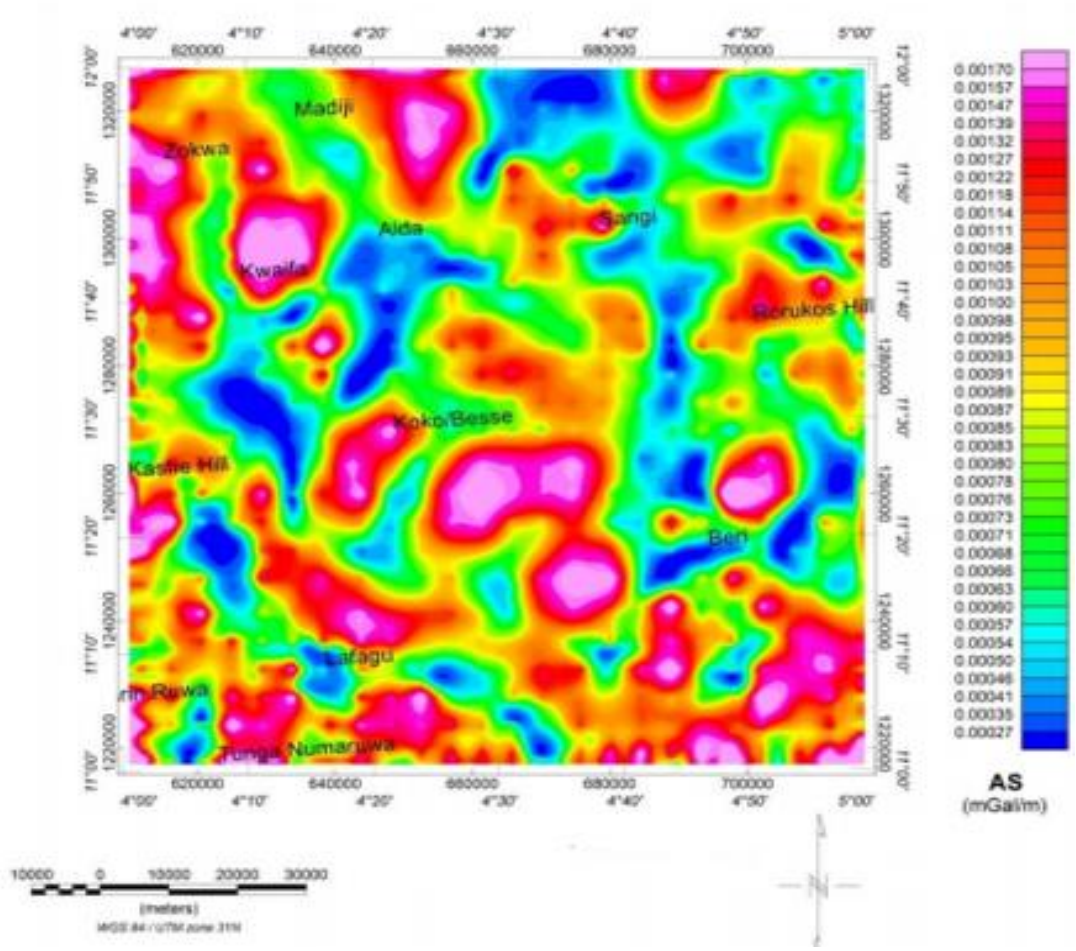


Figure 13: Analytic Signal Map of Parts of the study area

Structural Interpretation of Gravity Anomalies

The gravity derivative components of the field were computed by applying the Two-dimensional Fast Fourier Transform (2DFFT) directional filter on short wavelength anomalies (otherwise known as frequency anomalies; in this study referred to as residual anomaly fields) to weaken or attenuate long wavelength anomalies associated with deeply seated anomalies (Hesham and Heshan, 2016). The x (FHD-X) and y (FHD-Y) as first

EDITOR-IN-CHIEF
Prof. W. F. HILL [MALAWI]

horizontal derivatives as well as z (FVD-Z) first vertical derivative are calculated to hone, sharpen and improve the edges of potential anomalies signatures (Layade *et al*., 2020). The horizontal derivative is mathematically expressed in equation 27.0 as;

$$F = (ikx,y)^n F(\phi) \quad (27.0)$$

Where F represents the Fourier transform of the potential field; (^{n}) represents figure 1,2, the nth order horizontal derivative; ϕ= Potential of the field; (*ik,x y*) is an operator which transform a function into nth order derivative with respect to either x or y. The first vertical derivative is further expressed mathematically in equation 28.0 as;

$$F = K^n F(\phi) \quad (28.0)$$

The total horizontal and tilt derivatives play very significant roles in delineating shallow basement structures such as cracks, faults, fractures and lineaments. The total horizontal derivative is the arctan of the ratio of the vertical derivative to the horizontal derivatives (Falufosi and Oshinowo, 2021). FHD-X is the horizontal derivative of the gravity field along the X-direction, presented in **(**Figure 16). FHD-Y is the first horizontal derivative map of the gravity field along the Y direction presented in (Figure 15). The derivative techniques described which helped in producing the derivative grids are to aid the interpretation of geologic boundaries and other linear features of interest which serve as source of entrapments (Ferreira *et al.,*2011; Verduzco *et al*., 2004. Lines inferred on these maps where there are steep gradients and discontinuities are to make the linear features more visible (Layade *et al*., 2024).

The most significant benefit of derivative filter as applied to airborne gravity data is ability to delineate linear features (Dombrin and Savit, 1988) by enhancing discontinuities and anomaly textures as well as sharpening the edges of gravity anomaly textures over causative sources bodies. These linear features are structural deformations generally denoted as lineaments, faults, intrusive contacts, geological boundaries, joints etc., which may have been as a result of various tectonic events like subduction, terrain accretion and collision plates (Fitzsimons, 2016). The orientation of these linear features is found to be consistent with the regional texture pattern of Sokoto basin, adjacent to the main structural field patterns off (Figure 11) in the North-western parts.

First Vertical Derivative Map

The First Vertical Directional Derivative along the z-direction presented in (Figure 14) for the gravity revealed anomaly range of -0.00141 to 0.00107 mGal/m. The anomalies of the first vertical derivative along the z-direction were aligned along N-S trend vertically, the

EDITOR-IN-CHIEF
Prof. W. F. HILL [MALAWI]

anomalies or structures that trend in the same direction are from the same tectonic event as positioned by Omasanya *et al.*, 2012; while the regional effect of the total field have been attenuated.

First Horizontal Derivative Map

The First Derivative Map along the Y-direction presented in (Figure 15) for gravity revealed anomalies ranging from -0.00098 to 0.00091mGal/m. The anomalies of the first horizontal derivative along the Y-direction were aligned trending in the E-W and NW-SE directions. Literally, the anomalies were found to be trending in the same direction.

First Horizontal Derivative Map

The first horizontal derivative map along the direction presented in (Figure 16) for gravity outputs of parts of Sokoto basin revealed anomalies ranging from -0.00091 to 0.00090mGal/m. The anomalies of the first horizontal derivative along the X-direction were aligned with various structural deformations mapped in the study area, prominently trending NW-SE directions. Laterally, the anomalies were found trending in the same directions.

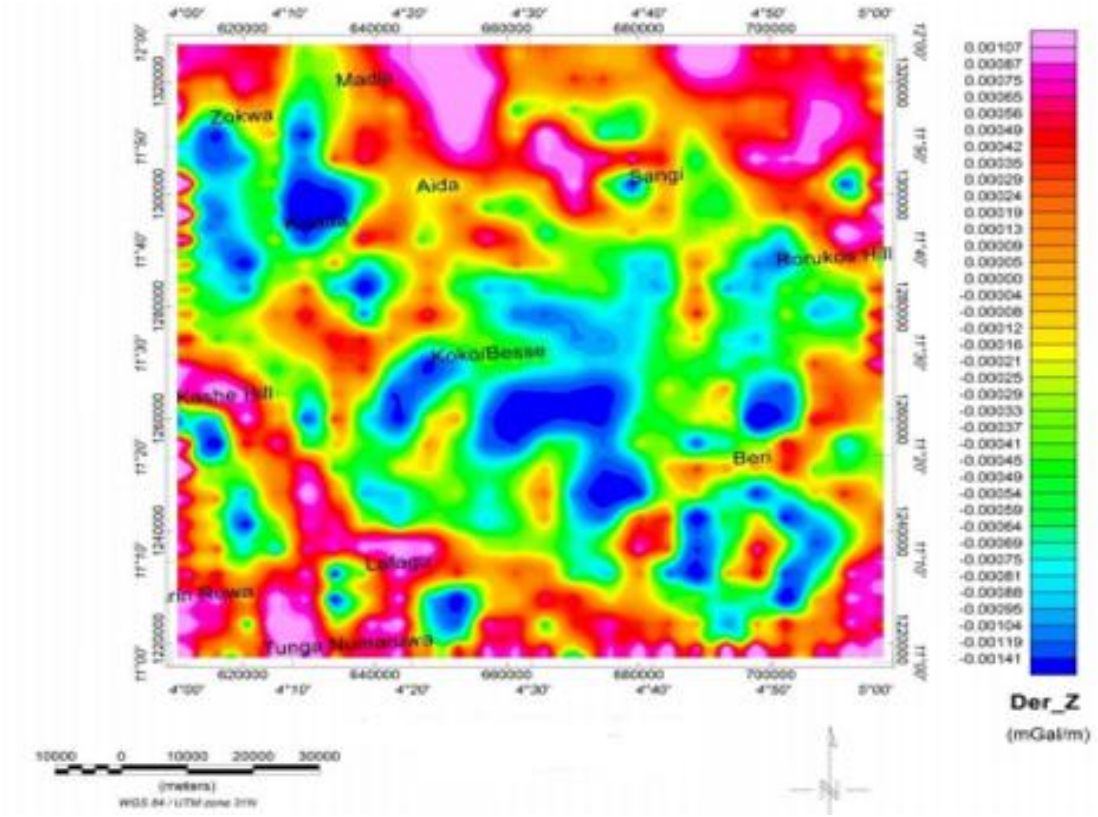


Figure 14: First Vertical Derivative Map of the study area (Along the Z-direction)

EDITOR-IN-CHIEF
Prof. W. F. HILL [MALAWI]

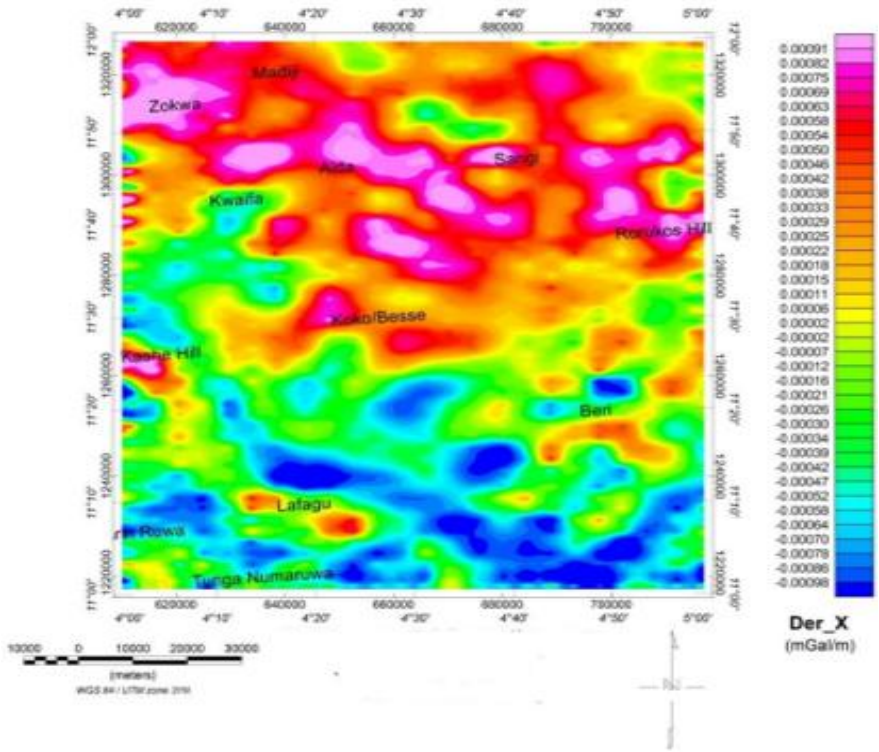


Figure 15: First Horizontal Derivative Map of the study area (along the Y-direction).

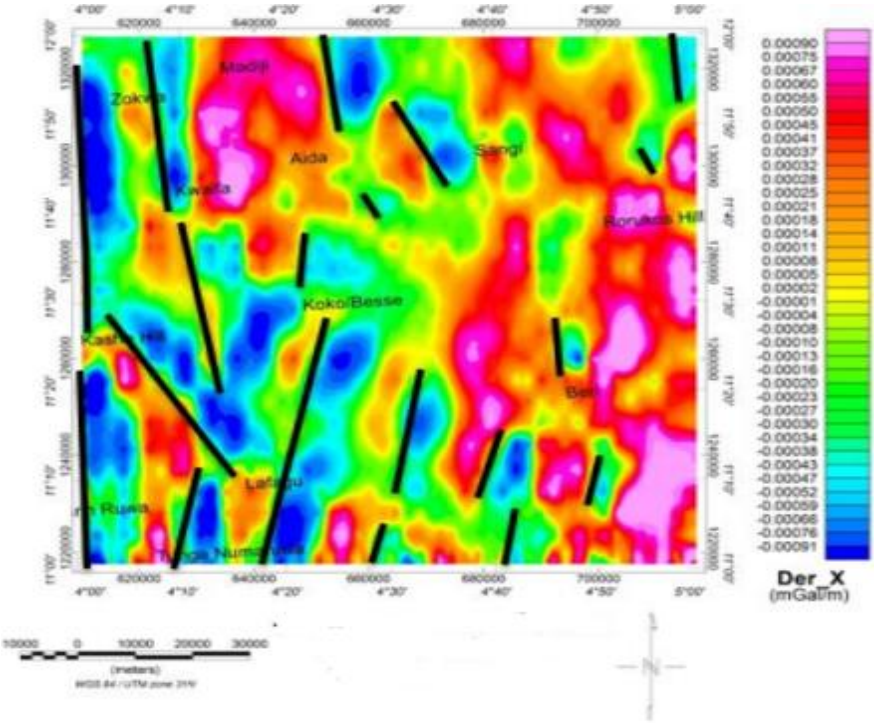


Figure 4.8: First Horizontal Derivative Map (Along the X-direction)

Quantitative Interpretation

The 3-D Euler deconvolution method was utilized to estimating the depth extent of the basin with regards to the basin with regards to the present anomalies' density in the study area. The 3D Euler Deconvolution method promised on a system of linear equations called ' homogeneity equation ' that relates the potential field and its gradient components to the position of the source with the degree of homogeneity η which is interpreted as a structural index, SI (Thompson, 1982). The 3-D form of euler's equation can be mathematically exposed as (Adegoke and Layade, 2019; Reid *et al*., 1990; Layade *et al*., 2024). Where x, y and z are the coordinates of a measuring point: $x_{\circ}$, $y_{\circ}$, and $z_{\circ}$ are the coordinates of the source location whose total field is detected as x, y and z; b is a base level: η is structural index (SI) and T is the total potential field. This method as developed by Thompson (1982) is based on functions governing potential field properties. The Euler deconvolution method was further developed and generated to suite a wider range of source types (geologic structures). The structural index (SI) for different potential source geometries (geologic models is summarized below in (Table 3).

The total field grid of gravity potential of the study area (Figure 9) with its respective directional derivative grids were used. The consistent review of past published literature as well as existing knowledge of regional and local geology of the investigated area were carefully guided and presented in the choice of parameters such as the grid interval (cell size, window size, structural indices, maximum/minimum distance, offsets, maximum/minimum location tolerance (and maximum depth tolerance. The minimize error in the depth computations and

Table 3: Structural Index for Geological Models (Thompson, 1982; Telford *et al*., 1998)

Geological Model	Number of Infinite Dimensions	SI for Gravity	SI for Magnetics
Sphere	0	2	3
Pipe	1 (z)	1	2
Horizontal Cylinder	1(X or Y)	1	2
Dyke	2 (Z and X or Y)	0	1
Sill	2 (X and Y)	0	1
Contact	3 (X, Y and Z)	0	0

To obtain the best possible results, is set to 15%, to 22%, x and y offsets to ±10m while the SI values of 0.0 was utilized for gravity potential field. The solution was therefore plotted using the zone-colored plot to have a 3D view of potential sources at varying depths. Although, other structural indices of gravity were tried on the solution whereas SI= 0 was

EDITOR-IN-CHIEF
Prof. W. F. HILL [MALAWI]

accepted to be the fairest solutions that represent the 3D Euler depth solution map of the study area presented in (Figure 17, 18, and 19) respectively as solution map of depth to gravity sources of S1=0, S2=1 and S3=2 respectively. The outputs of the solution of S1=0 for gravity potential field was only accepted after using S1 in the computations, as this structural index gave the fairest results in depth evaluation and lineation. Figure 17 is a fault structure that revealed a minimum depth range of 1483m to 2514m at an average of 2031m and a maximum depth range of 3632m to 6487m at an average depth of 6040m. Figure 18 is a typical horizontal cylinder with structural index S.I=1 that exhibited a minimum depth of less than 2000m with intermediate depth ranging from 2000m to 5000m, and 5000m to 10,000m while the maximum depth is exhibited to be greater than 10,000m. Figure 19 is a representation of a typical spherical geometric source of structural index (SI=2) that exhibited a minimum depth of less than 2500m and intermediate depth varying from 5000m to 7500m and 7500m to 10,000m while the estimated maximum depth is equally found to be greater than 10,000m. In addition, the observed maximum depth ranges revealed the depth locations of low frequency anomalies of gravity signatures of the study area. Also, the continuous elongation of contours observed on the Euler maps has direct implications for the predicted linear structures

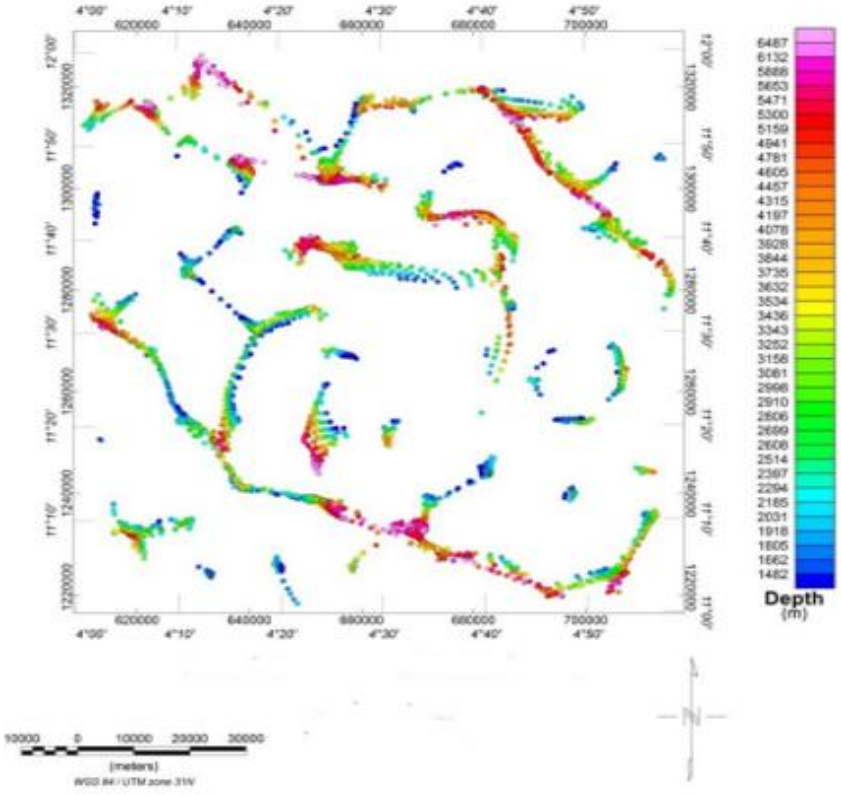


Figure 17: Euler Solution Map of the Study Area with SI=0 (Fault Structure)

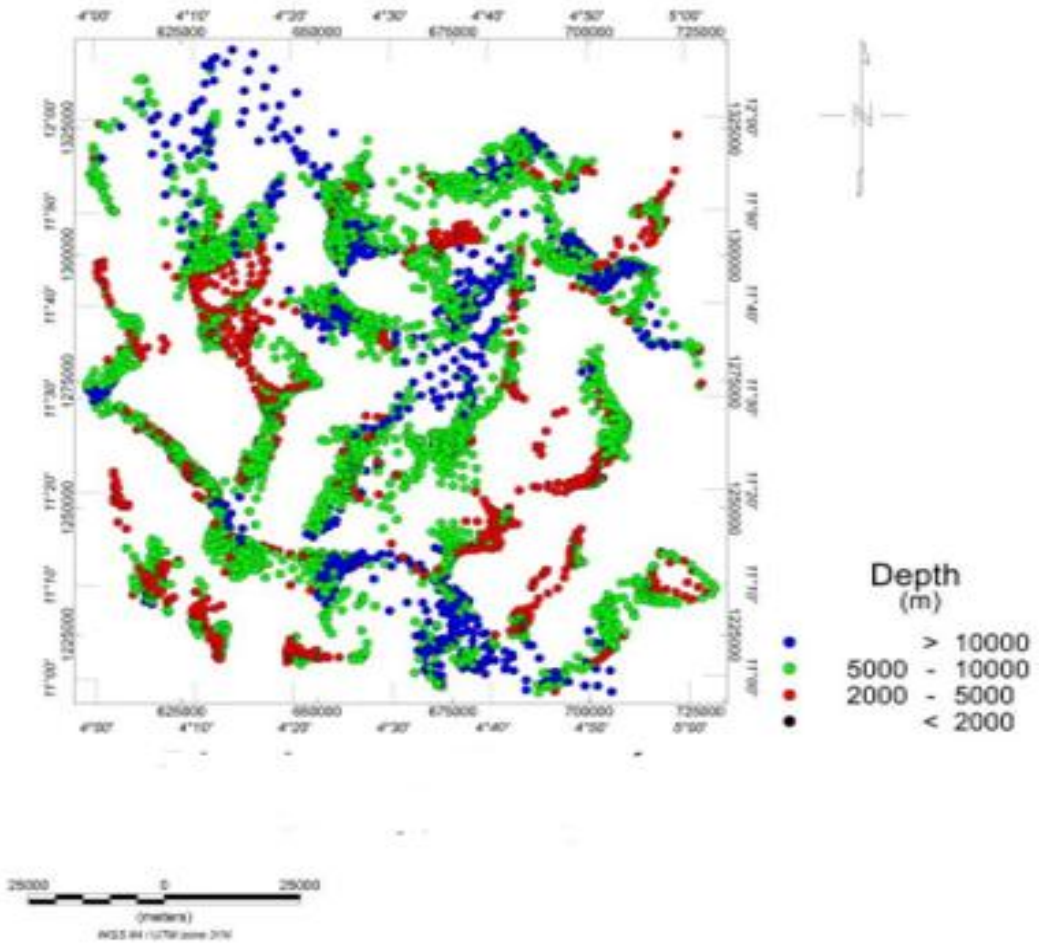


Figure 18: Euler Solution Map of the study area with SI=1 (Horizontal Cylinder)

In the investigated area. The observed thickness of the sedimentary cover as displayed from the Euler outputs is found to increase from east to west. Furthermore, since the data collected to tests for different source geometries namely fault, horizontal cylinders, and spheres which corresponds to structural indices of 0,1, and 2 respectively. Only the Euler solutions corresponding to source geometry of faults (Dyke/Sill/Faults) with SI=0 (Figure 17) can be utilized for making meaningful geologic interpretations as the clustering is not spurious unlike that corresponding to spheres and cylinders. These solutions are considered more appropriate because it contains less spurious solutions after windowing making geologically meaningful interpretation to be deduced from the map. The pattern continuous elongation of the contours around the South-East to the North-West parts conforms to the fault structures interpreted in the qualitative analysis. The blue/light blue coloration of the patterned contours interpreted as fault structures reveals that they were discovered at shallower depth compared to other structures while quantitative

comparison from 3D Euler Deconvolution revealed very close depth results as compared to the quantitative output. Moreso, the data clustering is a confirmation that the identified geologic structure that once appeared to correspond to the low-density contrast observed to be trending is the south-East to North-West in the study area is a fault. It is worthy of note that the presence of a fault is a potential source of conduits, entrapment reservoir for hydrocarbons and solid/ore minerals.

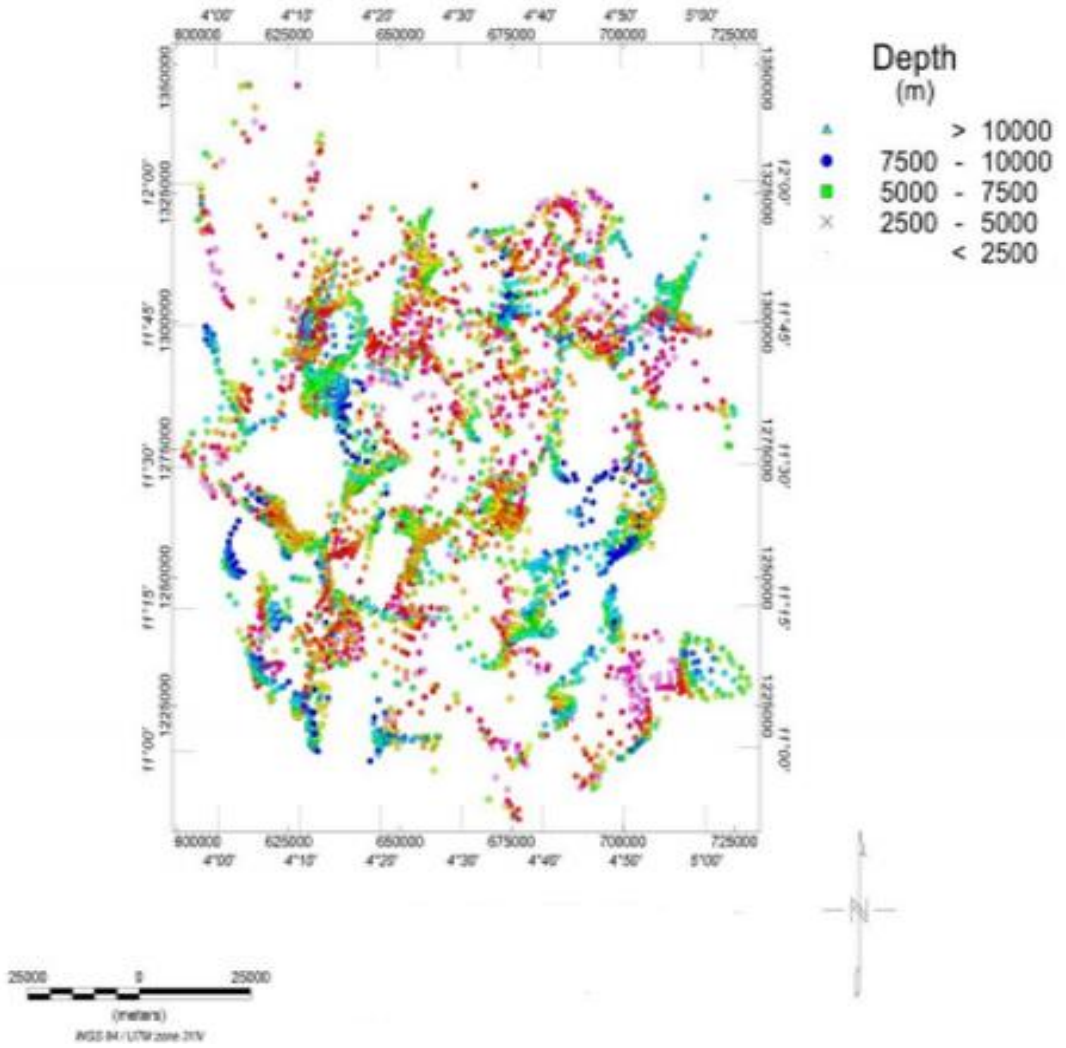


Figure 19: Euler solution map of the study area with SI=2 (Spherical Geometrics)

Depth Estimation and Structural Evaluation

Figure 17 of the Euler Solution Map with S.I =0 having maximum depth range of 5653m to 6487m and at an average 6040m (deep sources); and a minimum depth range of 1482m to 2514m at an average of 2032m (Shallow sources). The depth to basinal extent of gravity anomalous sources of parts of Sokoto basin evaluated in this study is a true

EDITOR-IN-CHIEF
Prof. W. F. HILL [MALAWI]

representation of the works of NGSA in and around the study area are in agreement with the results of this research. The depth range obtained can slightly hold prospects for hydrocarbon accumulation as positioned by (Abubakar and Likkason, 2022; Wright *et al.*,1985) that the minimum sedimentary thickness required for hydrocarbon exploration is 2300m while the elongation of the continuous plotted solutions confirms the presence of geologic structures like faults, dike and/or sill in the **s**tudy area. The minimum sedimentary thickness for solid minerals for exploring solid minerals and oil deposits varies significantly. In (Table 4); for oil production, it is typically 2 to 4km (1.2-2.5 miles) while for gas, it can range from 3-7km (1.9-4.3 miles), while for clastic-dominated mineral deposits often containing zinc, lead and other critical minerals require sedimentary basins when high thickness greater than 3km and up to 15km (1.9-4.3km miles) sequences of coarse clastic rocks in the likes of conglomerates, red beds and sandstones. However, other factors like the type of mineral, the geological settings and the tectonic history of the basin all play significant roles in determining the thickness of deposits.

Table 4: Depth Estimate from 3D Euler Deconvolution

Hydrocarbon/Mineral Exploration	Standard Depths	Current Study	Standard Depths
Oil	2000-4000m	Minimum (Shallow Structures)	1483-2514m
Gas	3000-7000m	Average (Intermediate structures)	2032m (shallow source) 6040m (deep source)
Ore Minerals Solid Minerals **(Pang *et al.*, 2015)**	>3000-15000m 150-800m 1000-7500m	Maximum (Deep structures)	5653-6487m

CONCLUSION AND RECOMMENDATIONS

The study focuses on assessing the hydrocarbon and solid mineral potential of the Sokoto Basin in Northwestern Nigeria using high-resolution airborne gravity data. The Sokoto Basin, part of the larger lullemmenden Basin, has undergone multiple depositional phases from the Cretaceous to Eocene represented by formations like the Gundumi, Illo, Rima, and Gwandu Formations. The Gwandu Formation, the youngest, is especially significant in Kebbi State. Due to the absence of deep exploratory wells in the basin, geophysical survey especially airborne gravity surveying was employed to investigate subsurface geological structures. The gravity method allows the identification of subsurface density variations,

EDITOR-IN-CHIEF
Prof. W. F. HILL [MALAWI]

structural features for hydrocarbon and mineral exploration. Data were analyzed using advanced filtering and depth estimation techniques like Fourier transforms, derivative mappings, and 3D Euler Deconvolution. Findings revealed gravity anomalies ranging from -28.26 to -71.67mgal. Density estimations showed a minimum basement depth of 1,412m and maximum of 6, 487m. Analytical map and derivative maps indicated fault zones, sills, and dykes that may acts as reservoir or traps. The analysis further revealed that the regional gravity values in the study area are predominantly negative, ranging from -52.37 to -54.98mgal. Derivative maps effectively delineated linear features such as faults and contacts, which align with N-S, E-W and NW-SE trends, indicating potential structural traps for hydrocarbons. Euler deconvolution results for a fault structure (SI=0) indicated depths ranging from a minimum of 1483 to 2514m, and a maximum of 3632to 6487m. Other structural models also suggested significant depths, with some exceeding 10,000m. A notable finding was the increasing thickness of the sedimentary cover from east to west across the basin. The presence of the mature cretaceous rock formations, coupled with identified structural traps, suggests a high potential for hydrocarbon generation and accumulation, especially in the southwestern and northwestern parts of the basin. However, the presence of magmatic intrusions and extensive faulting may present challenges to hydrocarbon preservation and migration. Overall, the study provides crucial geological insights that support further hydrocarbon exploration efforts in the Sokoto basin. Specialized geologic structures like Target structural traps and fault-bounded features should be specially investigated and areas that would be identified with structural traps like domal uplifts and faulted blocks should be prioritized for hydrocarbon exploration because domal features and intrusions could represent significant hydrocarbon reservoirs in traps. The deep lying anomalous gravity sources should be investigated for possible horst and graben structures which may signify extensional regimes that can create favorable conditions for hydrocarbon accumulation. These structures could form traps where hydrocarbons generated from deeper sources have migrated and accumulated. For this purpose, further geophysical studies including 3D seismic reflection surveys and exploration drilling should be conducted in all the areas identified with fault lines to validate the presence of hydrocarbons. The implementation of advance geophysical techniques such as high-resolution aeromagnetic surveys and 3D forward modelling can help in accurately mapping the extent and geometry of subsurface structures; this advanced scientific approach would provide a more precise characterization of potential hydrocarbon traps and mineral (solid and ore) rich zones thereby reducing exploration risks and costs. By leveraging this study findings, exploration companies can strategically target area with the highest potential for hydrocarbon and mineral deposits.

EDITOR-IN-CHIEF
Prof. W. F. HILL [MALAWI]

ACKNOWLEDGEMENTS

The author heartily acknowledges the Nigerian Geophysical Survey Agency (NGSA) for making the high resolution aerogravity data used for this research available. He is also highly thankful to the editor and anonymous reviewers who have helped improve this research.

REFERENCES

Abubakar, A. and Likkason, O.K. (2022). Exploring the Applications of Potential Field Gravity Method in Characterizing Regional-trends of the Earth Sequences system over the Sokoto basin, NW Nigeria. *Intech-Open Publication.* 1-20. https://dx.doi.org/10.5772/intechopen.102940

Adamu, A., Likkason, O.K., Maigari, A.S., and Ali, S. (2021). Structural mapping insight from gravity data for hydrocarbon accumulation in some parts of the Sokoto Basin, Northwestern Nigeria. In: 7th Assembly of Arab Conference on Astronomy and Geophysics (ACAG-7), Cairo, Egypt: *National Research Institute for Astronomy and Geophysics (NRIAG).* 11-14.

Adegoke, J.A. and Layade, G.O. (2019): Comparative depth estimation of iron-ore deposit using the Data-Coordinate Interpolation Technique for airborne and ground magnetic survey variation. *African Journal of Science, Technology, Innovation and Development (AJSTID)*. 11(5): 663-669. https://dx.doi.org/10.1080/20421338.2019.1572702

Adelana, S.M.A., and MacDonald, M.A.S (2008). Groundwater Research Issues in Africa. In: Groundwater Studies in Africa. *IAH Selected papers on Hydrogeology. London, New York, and Leiden: CRC Press, Taylor and Francis Group.* 13(1): 552-561.

Adelana, S.M.A., Olasehinde, P.I., and Vrbka, P. (2006). A quantitative estimation of groundwater recharge in parts of Sokoto Basin, Nigeria. *Journal of Environmental Hydrology*. 14(5): 11-17.

Adelana, S.M.A., Olasehinde, P.I., and Vrbka, P. (2005). Hydro-geological and Isotope research in the semi-arid area of Northeastern Nigeria. In: *Proceedings of the Biennial Groundwater Conference in Pretoria, Gauteng, South-Africa.* Division of the Geological Society of Southern Africa, CISR Conference Centre. 7-9.

Adeleye, D.R. (1974). Sedimentology of the fluvial Bida Sandstone (Cretaceous) Nigeria. *Sedimentary Geology* 12:1-24.

Adetona, A.A., Aliyu, S.B., Kwaghhua, F.I and Damidami, L.M. (2024). Groundwater investigation within the basement complex, North-Central Nigeria using Magnetic and Resistivity Method. *Arabian Journal of Geosciences*. 17(1): 6-20. https://doi.org/10.1093/jge/gxac055

Adewunmi, T. and Salako, K.A. (2018). Delineation of Mineral potential zone using high resolution aeromagnetic data over part of Nasarawa State, North Central, Nigeria. *Egyptian Journal of petroleum,* 27(4): 759-767.

Adimalla, N. (2019). Groundwater quality for drinking and irrigation purposes and potential health risks assessment: A case study from semi-arid region of South India. *Exposure and Health*. 11(1): 23-37. https://doi.org/10.1007/512403-018-0288-8

Adimalla, N. (2018). Spatial distribution, exposure, and potential health risk assessment for Nitrate in drinking water from semi-arid region, South India. *Francis and Taylor, Human and Ecological Risk Assessment: An International Journal*. 26(2): 310-334. https://doi.org/10.10890/10707309.2018.1508329

Ahmed, M.S., Tanko, A.I., Badamasi, W.H., Eduvie, M.O., and Abdulhamid, A. (2020). Groundwater vulnerability and risk assessment in Kaduna Metropolis, Northwest Nigeria. In: Witkouski, A.J., Jacbczyk-Karpiers, S (Zekaj, J, Grabula, D. *International Association of Hydrogeologists (IAH) Selected Papers (24).* London: CRC Press.

Ahmed, M.S., Tanko, A.I., Eduvie, M.O., and Ahmed, M. (2019). Assessment of Groundwater Vulnerability in Kaduna Metropolis, Northwest. *Nigeria. Journal of Geoscience and Environmental Protection*. 5(6): 115-131.

Ajibade, W.A., Ayodele, I.A. and Agbede, S.A. (2008). Water quality parameters in the major rivers of Kainji Lake National Park, Nigeria. *African Journal of Environment Science and Technology*. 2(7): 185-196.

Ajibade, A.C., Fitches, W.R. and Wright, J.B. (1979). The Zungerumylonites, Nigeria: recognition of a major tectonic unit. *Revue de geologiedynamiqueet de geographie Physique Paris.* 21(5): 359-363.

EDITOR-IN-CHIEF
Prof. W. F. HILL [MALAWI]

Akande, S.O, Ojo, O.J, Erdtman B.D, andHetenyi M. (2005). Paleoenvironments, organic petrology and Rock-Eval studies on source rock facies of the Lower Maastrichtian Patti Formation, Southern Bida Basin, Nigeria. *Journal of African Earth Sciences* 41(5): 394-406.

Akinegu, B.A., Chegbeleh, L.P., and Yidana, S.M. (2020). Characterization of groundwater flow and recharge in crystalline basement rocks in the Talensi District, Northern Ghana. *Journal of African Earth Sciences.* 161(1): 1215-1231. https://doi.org/10.1007/512517-023-11784-5

Akintoye, S.O., Adagunodo, T.A., Oladapo, M.I., Mimoh, E.A., Adebiyi, S.J., and Olayinka, A.I. (2023). Many gravity maps over Nigeria including the theoretical gravity map, absolute gravity map, and Bouguer gravity anomaly map to the geoid have been published. *Journal of Geophysics and Engineering*, 20(3), 455-470. https://doi.org/10.1093/jge/gxac055

Alagbe, S.O. (2006). Preliminary evaluation of hydro-history of the Kalambaina formation, Sokoto Basin, Nigeria. Environmental Geology. 51(1): 31-45.

Al-Amin, M.A. (2013). Energy production and Environmental concerns in Nigeria. The case of Kaduna Petroleum Refining on its host communities. *Journal of Energy Technologies and Policies*. 3(1): 69-77.

Anderson, H.R., and Ogilbee, W. (1973). Aquifers in the Sokoto Basin, Northwestern Nigeria with a description of the general hydrology of the region. *Water Supply Paper.* 1957-1979. https://doi.org/10.3133/wsp1757L

Arogundade, A.B, Hammed, O.S, Awoyemi, M.O, Falade, S.C, Ajama, O.D, Olayode, F.A, Adebayo A.S, and Olabode A.O. (2020). Analysis of aeomagnetic anomalies of parts of Chad Basin, Nigeria, using high-resolution aeromagnetic data. *Modelling Earth Systems and Environment.* 6(3):1545-1556.

Arseni, M., Wassouo-Elvis, B.N., Daniel, C., Theophile, N.M., Kelian, K., Daniel, N.J. (2018). Hydrogeophysical investigation for groundwater resources from electrical resistivity tomography and self- potential data in the Meighinga Area, Adamawa Cameroon. *International Journal of Geophysics.* 1(2): 35-51. https://doi.org/10.1135/2018/26975

Asiwaju-Bello, Y.A., Olabode, O.F., and Ogunsuyi, M.T. (2010). Pollution potential and causative hydrogeochemical processes in unconfined aquifer systems in a typical urban setting: emphasis on recharge and discharge areas. *Applied Water Science.* 10(1):52-71. https://doi.org/10.1007/s13201-019-1131-5

Awoyemi, M.O, Arogundade, A.B, Falade S.C, Ariyibi, E.A, Hammed, O.S, Alao, O.A, and Onyedim, G.C. (2016). Investigation of basement fault propagation in Chad Basin of Nigeria using high resolution aeromagnetic data. *Arabian Journal of Geosciences.* 9(6): 453.

Ayobami, I.O., and Theophillus, A.A. (2022). Groundwater source and flow in varying geological formations. IOP Conference Series: *Earth and Environmental Science*. 1197: 012009.

Barthelmes, F., and Kohler, W. (2016). International Centre for Global Earth Models (ICGEM). The Geodesists Handbook. In: *Journal of Geodynamics.* 90 (10): 907-1205. https://doi.org/10.1007/s00190-016-0948-z

Billman, H.G. (1992). Offshore stratigraphy and paleontology of Dahomey (Benin) Embayment. *NAPE Bull* 70 (2): 121-130.

BGS (2003). British Geological Survey in Groundwater Quality in Nigeria, Lagos. 8-9

Blakely, R. J. (1995). Potential Theory in Gravity and Magnetic Applications. A fundamental text explaining derivative filtering, including vertical derivatives, in potential field geophysics. *Cambridge University Press.* 23

Blakely, R. J. (1996). Potential Theory in Gravity and Magnetic Applications. Comprehensive text on potential field theory and analytical signal applications. *Cambridge University Press.* 34-45.

Carter, J.D., Barber, W., Tait, E.A. and Jones, G.P. (1963). The Geology of Parts of Adamawa, Bauchi and Borno Provinces in Northeastern Nigeria. *Geological Survey of Nigeria. Bulletin*, 30: 1-108.

Casas, A, Santolaria, P, Rivero, L, Casa-Sainz, A, Himi, M and Sendros, A. (2016). The gravity method: new challenges for delineation diapiric structures in North-East Spain. *First break* 34(8).

Dada, S.S. (2008). Proterozoic evolution of the Nigeria-Boborema province. *Geological Society, London, Special Publications*, 294(1): 121-136.

EDITOR-IN-CHIEF
Prof. W. F. HILL [MALAWI]

Dailalos, S., Alexopoulos, J.D and Lozios, S. (2019). New insights on subsurface geological and tectonic structure of the Athens basin, Greece derived from urban gravity measurements. *Journal Application of Geophysics*. 167(1): 73-105.

Dankwo, L.C and Lar, U.A. (2013). Hydro-electric characteristics of Upper River Shemakar Basin, Jos Plateau: A case study of Jobam and Environs. *International Organization of Scientific Research (IOSR), Journal of Applied Geology and Geophysics*. 1(5): 47-57. http://dx.doi.org/10.979010990-0154757

Digital Elevation Model (2006). Topography Map of Latitude 11° 30ˈN - 13° 30N and Longitude 4° 00ˈE - 6° 00ˈE.

Dombrin, M.B, Savit, C.H. (1988). Introduction to geophysical prospecting, 4th Edn. *McGrawHill, New York.*

Doust, H. and Omatsola, E. (1990). Niger-Delta. In: Edwards JD, Santo-grossi P. A (eds) Divergent/passive margins basins. *AAPG Memoir*. 48: 201-238.

Edmunds, H.M., Fillman, E., and Goni, I.B. (1991). Lake, groundwater and paleohydrology in the Sahel of Northeastern Nigeria. Evidence from hydrogeochemistry. Geological Society of London. *Journal of the Geological Society of hydrogeochemistry*. 156(1): 345-355.

Edunjobi, H.O, Layade, O.G, Makinde, V, Bada, B.S, Ogunbayo A.F, and Atunrase, K.A. (2023). Qualitative interpretation of high-resolution aeromagnetic data of Abeokuta Metropolis for geological characterization. *Result in Geophysical Sciences* 15, 100062.

Ekwueme, O.U, Obiora, D.N, Igwe, E.A, Abangwu, J.U. (2018). Study of aeromagnetic anomalies of Idah and Angba areas, North central Nigeria, using high resolution aeromagnetic data. *Modelling Earth Systems and Environment* 4(2): 461-474.

Ellumali, V., Drindha, K., Sithole, B., and Laskshmanami, E. (2017). Spatial interpolation methods and geostatistics for mapping groundwater contamination in a coastal area. *Environmental Science and Pollution Research.* 24(3): 115-132. https://doi.org/10.1007/s11356-017-8681-6

Emere, M.C., and Dibal, D.M. (2003). Metal accumulation in some tissues/organs of a freshwater fish (clarias garie penus) from some polluted zones of River Kaduna. *Journal of Biology, Agriculture and Healthcare.* 3(1): 213-228.

Emujakporue, G, Ofoha, C.C, and Kiani, I. (2017). Investigation into the basement morphology and tectonic lineament using aeromagnetic anomalies of parts of Sokoto basin, Northwestern, Nigeria. *Egyptian Journal of Petroleum* 27(4): 11. https://dx.doi.org/10.10.1016/j.ejpe.2017.10.003

Ette, O.J., Okuofo, C.A., Adie, D.B., and Igboro, S.B. (2017). Suitability of water from the continental terminal of Sokoto Basin in Northwestern Nigeria for Irrigation. *Journal of Occupational Safety Environment and Health*. 4(1): 1-9.

Falufosi, M.A and Osinowo, O.O. (2021). Evaluation of basement topography and structures in the Dahomey Basin and surrounding environs of Southwestern Nigeria, using satellite gravity data. *NRIAG Journal of Astronomy and Geophysics*. 10(1): 333-346.

Falconer, J.D. (1911). The geology of the Jos plateau. *Geographical Journal*, 38(5): 481-496.

Ferreira, J.F, De Castro, G.L, Bongiolo, B.S, De Souza, J, and Romeiro, A.T. (2011). Enhancement of the Total Horizontal Gradient of Magnetic Anomalies using Tilt Derivatives*: Part 11-Application to Real Data*. SEG-2011-0887.

Fhyn, M.BW, Peterson,H.I, Mathiesen, A, Nielson, L.H, Pedersen, S.AS, Lindstrom, S, Bojesen-Kefoed, J.A, Abatzis, L, and Boldreel, L.O (2010). Vietnamese sedimentary basins: geological evolution and petroleum potential. *GUES Bulletin* 20: 91-94.

Fitzsimons, CW Ian. (2016). Pan-African granulites of Madagascar and southern India; Gondwana assembly and parallels with modern Tibet. *Journal of Mineralogical and Petrological Sciences* 111 (2): 72-88.

FMWRRD (1995). Federal Ministry of Water Resources and Rural Development on the study of the Natural Water Resources Master Plan. Federal Republic Nigeria, Abuja. Japan International Corporation (JICA) and Federal Ministry of Water Resources and Rural Development. *FMWRRD Bulletin.* 56-59.

Freeze, D and Barber, W. (1965). The distribution and chemical quality of groundwater in Northern Nigeria. *Geological Survey of Nigeria (GSN)*. In: *GSN Bulletin.* 36(1): 1-20.

EDITOR-IN-CHIEF
Prof. W. F. HILL [MALAWI]

Garba, I. (2002). Geochemical characteristics of the gold mineralization near Toshon, Birnin-Gwari, Northern Nigeria. *Geochemistry* 62 (2): 160-170.

Gilardoni, M., Reguzzoni,M., Sampietro, D.(2016). GECO Global gravity model by locally combining GOCE data and EGM2008. *Stud Geophysaical and Geodynamkics.* 60(2): 228-247.

GOM (2014). Geosoft Oasis Montaj in data processing and analysis systems for earth science applications (Version 8.4). *Geosoft Incorporated, Toronto*, Canada. www.geosoft.com

Goodenough, K.M., Lusty, P.A.J., Roberts, N.M.W., Key, R.M. and Garba, A. (2014). Post-collisional Pan-African granitoid and rare metal pegmatites in Western Nigeria: *Age, Petrogenesis, and the Pegmatite conundrum*. Lithos, 200: 22-34.

Graham, D. W., Jones, K., & Milligan, P. R. (2014). Digital data processing for airborne geophysical images. *Exploration Geophysics*, 45(2): 79-88.

Graham, K.M., Preko, D.D., Wemegah, W and Boamah, D. (2014). Geological and Structural Interpretation of Part of the Buem Formation, Ghana using Aeromagnetic Data. *Journal of Environment and Earth Science.* 4(4): 17-31.

Grant, N.K. (1978). Structural distinction between a metasedimentary cover and underlying basement in the 600-my-old Pan-African domain of northwestern Nigeria, West Africa. *Geological Survey of America Bulletin*, 89(1): 50-58.

Hackney,R.L., and Featherstone, W.E.(2003). Geodetic versus geophysical perspectives of the gravity anomaly. *Geophysical Journal International.* 154(1): 35-41.

Hesham, S.Z, and Hesham, T.O. (2016). Application of High-Pass Filtering Techniques on Gravity and Magnetic Data of the Eastern Qattara Depression Area, Western Desert, Egypt. *National Research Institute of Astronomy and Geophysics*. 5(1): 106-123.

Ibim, D.F.; Amaechi, C. J; B. Nwinka and A.A. Agogo (2025). Gravity and magnetic techniques for the delineation of subterranean structural features of the basement complex, Imo River-Basin, Southeastern Nigeria. 15(1): 4461- 4780.

Ibrahim, H.A., Abdulkarim, M., Grema, H.M., Abdullahi, M.I., and Hamidu, H. (2020). Physico-chemical assessment of water quality in the Gidan-Gulbi shallow floodplain aquifer, Northwestern Nigeria. *American Journal of Water Resources.* 8(4): 155-163. https://doi.org/10.12691/ajwr-8-4-1

Ikeri, H.I. (2021). Interpretation of Aeromagnetic Data of Guzabure and its Environs, Chad Basin of Northeastern Nigeria using Source Parameter Imaging. *International Journal of Engineering Sciences.* 10(5): 11-21.https://doi.org/10.9790/1813-1005034550

IOSHIC (1999). International Occupational Safety and Health Information Centre; Basics of Chemical Safety: In IOSHIC Report. *Labour Organization Conference.* Geneva, Switzerland. 23-25.

Joseph, I.A. (2015). Threats to water resources development in Nigeria. *Journal of Geology and Geophysics.* 4(1): 205-2011.

Ishola, S.A., Akinyemi, A.M., Edunjobi, H.O., Kuforiji, H.I., Ogunkoya, C.O and Babalola, Q. (2026). Depth Estimation of Causative Bodies using Euler Deconvolution Technique in Parts of Sokoto Basin, North-West Nigeria. *Harvard Research and Publications International, International Journal of Environmental Design and Construction Management (IJEDM).* 11(4): 86-113.

Ishola, S.A., and Akinyemi, A.M. (2025). Characterizations and Delineations for Hydrocarbons and Solid Mineral Potentials using High Resolution Airborne Gravity Data in parts of Sokoto Basin, Northwestern Nigeria. 2025 *Undergraduate Research Project, Department of Earth Sciences, Olabisi Onabanjo University, Ago-Iwoye*. 1-129.

Ismail, A.M, Sultan, S.A, and Mohamady, M.M. (2001). Bouguer and total magnetic intensity maps of Sinai Peninsula, Scale 1:500,000. In: Proc. 2nd *International Symposium on Geophysics, Tanta*. 111-117.

Jones, H.A and Hockey, R.D. (1964). The Geology of Parts of Southwestern Nigeria, *Geological Survey of Nigeria Bulletin*, 31:87.

Kamureyina, E, Omang, B.O, Kasidi, S, Owolabi, A.O, and Nur, A. (2019). Determination of Hydrocarbon Potentials Using High Resolution Aeromagnetic Data Over Sokoto Basin, Northwestern Nigeria. *International Journal of Geosciences* 10: 419-438. https://doi.org/10.4236/ijg.2019.104024

EDITOR-IN-CHIEF
Prof. W. F. HILL [MALAWI]

Karpik, A.P., Kanushin, V.F., Ganagina, I.G., Goldobin, D.N., Kosarev, N.S., Kosarev, A.M. (2016). Evaluation of recent earth's global global gravity field models with terrestrial gravity data. *Contribution Geophysical Geodynamics*. 123(4): 1-11.

Kasidi, S, and Yusuf, S.N. (2019). Determination of Hydro Geological and Petroleum Potential using High Resolution Aeromagnetic Data, Over Katsina and Environs, Parts of Nigeria Sector of Chad Basin, North. *Journal of Geography, Environment and Earth Science International.* 23(1):1-12.

Kayan, K.R. (2008). Potential theory in Applied Geophysics. Springer, Heidenberg, New-York.

Kearey, P, Brooks, M, and Hill,I . (2002). An Introduction to Geophysical Exploration. *Oxford: Blackwell Publishing* 3rd Edition.

Kogbe, C.A. (1979). Geology of Southeastern Portion of the Ilullemmeden Basin (Sokoto Basin). Zaria, Nigeria: *Bulletin of the Department of Geology, Ahmadu Bello University*; 420.

Kogbe, C.A. (1981). Cretaceous and Tertiary of the Ilullumenden Basin in Nigeria (West African). *Cretaceous Research;* 2: 129-186.

Kogbe, C.A. (1989). The Cretaceous and Paleogene sediments of southern Nigeria. *Geology of Nigeria* 2: 325-334.

Kroner, A., Ekwueme, B.N. and Pidgeon, R.T. (2001). The oldest Rock in West Africa: SHRIMP Zircon Age for Early Archean Migmatitic Orthogneiss at Kaduna, Northern Nigeria. *The Journal of Geology*. 109: 399-406. http://dx.doi.org/10.1086/319979.

KSG (2014). Kebbi State Government on Historical Review and Resources of Kebbi State. Gwadanggaji Secretariat, Birnin-Kebbi, Kebbi State. www.kebbistate.gov.ng ; info@kebbistate.gov.ng

Khazari, D and Gabtni, H. (2018). Geophysical methods integration for deep aquifer reservoir characterization and modelling in Sidi-Bouzid Basin, Central Tunisia. *Journal of African Earth Sciences*. 138: 289-308.

Kwaya, M.Y., Hamidu, H., Abdullahi, I.M., Yelwa, N.A., I Abdulganiyu, Y., Kana, A.M., Ibrahim, H.A., and Grena, H.M. (2020). Irrigation and drinking groundwater quality indices of Gada community and Environs, Semi-arid region, Sokoto Basin, Northwestern Nigeria. *Nigerian Journal of Science.* 54(1): 85-103.

Kwaya, M.Y., Hamidu, H., Abdullahi, I.M., Yelwa, N.A., Ibrahim, H.A., Abdulganiyu, V., and Mohamed, D. (2019). Hydrogeochemical characterization and multivariate statistical assessment of Gada town and its surroundings, Iullemmeden Basin, Northeastern Nigeria. *Science Forum, Journal of Pure and Applied Science.* 19(1): 109-120. https://doi.org/10.5455/sf.57745

Layade, G, Adewumi, O, Makinde, V, and Bada, B. (2021). Application of Gravity Survey for the Investigation of the Presence and Depth of Iron-ore Deposit. *Petroleum and Coal*, 63:577-588

Layade, G. O, Edunjobi, H. O, Makinde, V, and Bada, B.S. (2020). Estimation of Depth to Bouguer Anomaly sources using Euler Deconvolution Techniques. *RMZ-M & G/2020/Vol.*671(1):185-195. http://dx.doi.org/10.1086/319979.10.2478/rmzm&g-2020-0016

Layade, G.O, Adegoke, J.A, Adefemi, F.O, and Edunjobi, H.O. (2023). Source Parameter Imaging and 3D Euler Deconvolution method for the Determination of Geometry and Estimating Depth of Agbadu Bituminous sand*: Petroleum and Coal.* 65(3): 933-945.

Layade, G.O, Edunjobi, H.O, and Ajayi, K.D. (2024). Lineament Qualitative Interpretation and Depth Evaluation of Potential Field Signatures in the Abeokuta Region, Southwestern Nigeria. *Journal of the Earth and Space Physics* 49(4): 37-55. 10.22 http://dx.doi.org/10.22059/jesphys.2023.358877.10075

Likkason, O.K., Maigari, A.S., and Ali, S. (2014). Mapping of features related to hydrocarbon and other mineralization potentials of Southeastern Sokoto Basin, North-West Nigeria by using High-Resolution Aeromagnetic Data. *Arabian Journal of Geoscience*. 17(1): 216. http://dx.doi.org/10.1007/s12517-024-12018.y

Maduabuchi, C., Maloszewski, P., Stichler, W., and Eduvie, M. (2003). Preliminary interpretation of environmental isotope data in the Chad basin aquifers. In: *Northeastern Nigeria International Symposium on Isotope Hydrology and Integrated Water Resources Management*. Vienna, Austria. 19-23

Martinez-Moreno,F.J, Galindo-Zaldivar, J, Pedrera, A, Teixido, T, Pena, J.A and Gonzalez-Castillo. (2015). Regional and residual anomaly separation in microgravity maps for cave detection: The case study of Grute de las Maravillas (SW Spain). *Journal of Applied Geophysics* 114: 1-11.

McCurry, P. (1976). The Geology of the Precambrian of Lower Paleozoic Rocks of Northern Nigeria. *A Review*. 11.

Megawata, U.Z., Olasunkanmi, N.K., Egbeyale, G.B., and Saleh, A. (2025). Structure and Mineralization Potential of the Southern Basin in Nigeria. *Frontier Earth Sciences.* 13(1): 121-135. http://dx.doi.org/10.3389/feart.2025.1500162

Mickus, K. (2004). The gravity method in engineering and environmental applications. In: *Federal Highway Administration and Florida Department of Transportation Special Publication*. 11-24.

Morton, A. (2015). Universal Transverse Mercartor Grid Zone of the World. In: Atlas Florae Europaeae. UTM and MGRS/ Transverse Mercartor Calculator. www.dmap.co.uk.utmworldhtm

Nabighian, M.N. (1972a). Towards a three-dimensional automatic interpretation of potential field data via generated Hilbert transforms: fundamental relations. *Geophysics*. 49(1): 780-786.

Nabighian, M.N. (1972b) The Analytic Signal of Two-Dimensional Magnetic Bodies with Polygonal Cross-Section: Its Properties and Use for Automated Anomaly Interpretation. *Geophysics,* 37(1): 507-517.

Naidu, P. (1968). Spectrum of the potential field due to randomly distributed sources. *Geophysics.* 33(2): 337-345.

Ndougsa-Mbarga, T., Manguelle-Dicoum, E., Campos-Enriquez, J., and Atangana, Q.Y. (2007). Gravity anomalies, sub-surface structures and oil and gas migration in the Mamfe, Cameroon-Nigeria, Sedimentary basin. *Geofisca International.* 46(2):129-139.

Nettleton, L.L. (1976). Regionals, residuals and Structures. Geophysics. 19(1): 1-22.

NGSA. (2006). Nigerian Geological Survey Agency. Mineral Resources Map of Nigeria. 1map scale 1:2000,000.

NGSA (2005), Nigeria Geological Survey Agency (NGSA). Airborne Geophysical Digital Data Dissemination Guideline.

NGSA (2017), Nigeria Geological Survey Agency (NGSA) Manual. In: High Resolution Airborne Geophysical Survey. 23-25.

NSDWQ (2015). Nigerian Standard Water Quality in Nigerian Industrial Standard. 554:30-32.

Nura, A.Y., Hamidu, H., Kana, M.A., Usman, A., and Falalu, B.H. (2018). Spatial distribution of groundwater resources of the continental terminal aquifers Sokoto Basin, Northwestern Nigeria. Ahmadu Bello University, Zaria. *Journal of Scientific Research, Faculty of Life Sciences*. 17(2): 174-187.

Nwajide, C.S. (2013). Geology of Nigeria's sedimentary basins. *CSS Bookshop Limited.*

Nwankwo, C and Ekine, A. (2009). Geothermal gradients in the Chad Basin, Nigeria, from bottom hole temperature logs. *International Journal of Physics Sciences.* 4(12): 777-783.

Nwankwo, C.N, Emujakporue, G.O, and Nwosu, L.I. (2012). Evaluation of the petroleum potential and prospects of the Chad Basin Nigeria from heat flow and gravity data. *Journal of Petroleum Exploration and Production Technology.* 2(1): 1-6.

Obaje, N.G., Faruq, M., Burai, A., Moses, S.D., Ali, M., Adamu, S., Essien, A., Lamorde, U., Umar, U.M., Ozogi, T.M., Okonkwo, P., Lukman, M., Idris, A.I., Faruq, Z., and Umar, M. (2020). A short note on the Petroleum Potentials of the Sokoto Basin in Northwestern Nigeria. *Petroleum Science and Engineering*. 4(1): 34-38. http://dx.doi.org/10.11648/j.psc.2020401.14

Obaje, N.G., Attah, D.O., Opeloye, S.A. and Moumouni, A. (2006). Geochemical evaluation of the hydrocarbon prospects of sedimentary basins in Northern Nigeria. *Geochemical Journal*. 40(3): 227-243.

Obaje, N.G, Aduku M, and Yusuf I. (2013). The Sokoto Basin of Northwestern Nigeria: A preliminary assessment of hydrocarbon prospectivity. *Petroleum Technology Development Journal.* 3(2): 66-80.

Obaje, N.G. (2009). Geology and Mineral Resources of Nigeria: *Lecture Notes in Earth Sciences.* Berlin Heidelberg: Springer.

EDITOR-IN-CHIEF
Prof. W. F. HILL [MALAWI]

Obaje, N.G, Bomai, A, Moses, S.D, Ali, M., Aweda, A., Habu, S.J, Idris-Nda, A., Goro, A.I, and Wazir, S. (2020). Updates on the geology and potential petroleum system of the Bida Basin in Central Nigeria. *Petroleum Science and Engineering* 4(1): 23-33.

Obiora, D.N., Ossai, M.N., Okeke, F.N., and Oha, A.I. (2016). Interpretation of airborne geophysical data of Nssuka area, Southeastern Nigeria. *Journal of the Geological Society of* India. 88(1): 654-667.

Ogbodu, P.A, Okon, E.E, Ugar, S.I, Lebo, S.E, Alo, G.A and Okereke, S.S. (2025). Sediment thickness distribution and 2D Depth model of the Ikom Basin, Southeastern Nigeria, using high resolution aeromagnetic data. *Global Journal of Pure and Applied sciences.* 31(1): 225-232.

Ojo, S.B. and Ajakaiye, D.E. (1989). Preliminary Interpretation of Gravity Measurements in the Middle Niger Basin Area, Nigeria. In: Kogbe, C.A., Ed., Geology of Nigeria, 2nd Edition, *Elizabethan Publishing Company, Lagos,* 347-358.

Ojoh, K.A. (1992). The southern part of Benue Trough (Nigeria) Cretaceous stratigraphy, basin, paleo-oceanography and geodynamic evolution in the Equatorial domain of the South Atlantic. *NAPE Bulletin.* 7(2): 131-152.

Okpoli, C.C, and Akingboye, A.S. (2019). Application of high-resolution gravity data for litho-structural and depth characterization around Igabi area, Northwestern Nigeria. *NRIAG Journal of Astronomy and Geophysics.* 8(1): 231-241.

Olade, M.A. and Elueze, A.A. (1979). Petrochemistry of the Ilesha amphibolites and Precambrian crustal evolution in the Pan-African domain of South-West Nigeria. *Precambrian Research* 8(3-4): 303-318.

Omasanya, K.O, Akinbodewa, A.E, and Mosuro, G.O. (2012): Integrated Mapping of Lineament in Ago-Iwoye SE, SW Nigeria, *International Journal of Science Technology*. 1(2): 68-79.

Omatsola, M.E and Adegoke, O.S. (1981) Tectonic Evolution and Cretaceous Stratigraphy of the Dahomey Basin. *Nigeria Journal Mining and Geology.* 18(1): 130-137.

Onyeche, I.N, Ombu, R., and Eke, P.O. (2023). Application of Gravity method in determination of hydrocarbon potentials in parts of the Anambra Basin, Southwestern Nigeria. *Faculty of Natural and Applied Sciences Journal of Scientific Innovations.* 4(1):198-210.

Osazuwa, I.B. (1991). Method of execution and analysis of observations of the primary gravity network of Nigeria. *International Journal of Bio-Chemi-Physics.* 1(2):30 36

Osazuwa, I.B. (1988). Cascade Model for the removal of drift from gravimetric data. *Survey Review*. 299228): 295-303.

Osinowo O.O, and Olayinka, A.I. (2013). Aeromagnetic mapping of basement topography around the Ijebu-Ode geological transition zone, Southwestern Nigeria. *Acta Geodaetica et Geophysics.* 48(4): 451-470.

Oteze, G.E. (1991). Portability of groundwater from Rima Group aquifers in the Sokoto Basin. *Nigerian Journal of Mining Geology.* 27(1): 17-23.

Oteze, G.E. (1976). The hydreogeology of North-Western Nigerian Basin. In: Kogbe, C.A. Geology of Nigeria *Elizabethan Publishing Company,* Ibadan, Nigeria.

Otlaandosa, T., Ranganai, R.T., Ditiro, B.M., Kealeboga, K.M., and Joyce, G.M. (2022). Investigating groundwater recharge potential of Notwane Catchment in Bostwana using Geophysical and Geospatial tools. *Regional Study-Journal of Hydrology.* 40(1): 101-119. https://doi.org/10.1016/j.ejrh.2022.101011

Oyawoye, M.O. (1972). The basement complex of Nigeria. *African Geology*. 67-99.

Pang, X, Jia, C and Wang, W. (2015). Petroleum geology features and research developments of hydrocarbon accumulation in deep petroliferous basins. 12(1): 1-53.

Pavlis, N.K., Factor, J.K., and Holmes, S.A. (2007). Terrain-related gravimetric quantities computed for the next EGM. Proceedingsof the 1st International Symposium of the International Gravity Field Service. *Journal Map* (Special Issue). 18: 318-323.

Petters, S.W. (1978). Stratigraphic evolution of the Benue Trough and its implications for the Upper Cretaceous Paleogeographic of West Africa. *The Journal of Geology* 86(3): 311-322.

EDITOR-IN-CHIEF
Prof. W. F. HILL [MALAWI]

Petters, S.W, and Ekweozor, C.M. (1982). Petroleum geology of Benue trough and southeastern Chad basin, Nigeria. *AAPG Bulletin* 66(8): 1141-1149.

Phillips, J.D., Saltus, R.W., and Reynolds, R.L(1998). Sources of Magnetic Anomalies over a sedimentary Basin-Preliminary results from the coastal plain of the Arctic National Wildlife Refuge, Alaska in Gibson, R.J., and Milligan, P.S (Eds), Geologic Applications of Gravity and Magnetics: Case Histories: *Society of Exploration Geophysicists and American Association of Petroleum Geologists*. 130-134.

Rahaman, M.A. (1976). Review of the Basement Geology of Southwestern Nigeria. *In Precambrian Geology of Nigeria, Geological Survey of Nigeria*. 41-58.

Rahaman, M.A. (1981). Migmatites and Associated Rocks in the Nigerian Basement Complex. *Precambrian Research,* 15(3): 251-274.

Rahaman, M.A. and Lancelot, J.R. (1984). Continental crust evolution in southwestern Nigeria: constraints from U/Pb dating of Pan-Africa Gneiss. *Earth Planets Science Letter*, 67(1): 19-34.

Rahaman, M.A. (1988). Recent Advances in the Study of the Basement Complex of Nigeria. *Journal of African Earth Sciences (and the Middle East),* 7(1- 2): 307-332.

Rahaman, M.A., and Ocan, O. (1988). The nature of the boundary between the schist belts and the basement complex rocks in the Ilesha area, Southern Nigeria. *Journal of African Earth Sciences*. 6(2): 153-163.

Reid, A.B. Ebbing, J, and Webb, S.J. (2014). Avoidable Euler errors- the use and abuse of Euler deconvolution applied to potential fields. *Geophysics* Prospecting. 62 (5): 1162-1168.

Reid, A. B., Allsop, J. M., Granser, H., Millett, A. J., and Somerton, I. W. (1990). "Magnetic interpretation in three dimensions using Euler deconvolution. 3D Euler Deconvolution for gravity and magnetic applications." *Geophysics.* 55(1): 80–91.

Reeves, J. (2005). Advancing New 3D Seismic Interpretation Methods for Exploration and Development of Fractured Tight Gas Reservoirs. *Geo-Spectrum Incorporated.*

Salawu, N.B, Orosun, M.M, Adebiyi, L.S, Abdulraheem, T.Y, Dada, S.S. (2020). Existence of subsurface structures from aeromagnetic data interpretation of the crustal architecture around Ibi, Middle Benue, Nigeria. *SN Applied Sciences* 2(3): 427.

Sayad, M.M., Rahim, S; and Tahr, T. (1998). Chemistry of groundwater of Rawalpindi/Islamabad. In: Proceedings of Water Engineering and Development Centre (WEDC) in "*Sanitation and Water for All'. 24th Conference, Islamabad,* Pakistan.

Sfada, A.S. (2025). Magnetic Data Analysis for Estimations of Depth to Basement and Structural framework of Dinawa and Surroundings, Sokoto Northwestern Nigeria. *Geosciences Research.* 3(2): 1-7. https://doi.org/10.26480/gsrj.02.2025.57.63

Smith, D. (2007). The GRAV-D Project: Gravity for the redefinition of the American Vertical datum. *ANOAA contribution to the Global Geodetic Observing System (GGOS) component of the Global Earth Observation System of Systems (GEOSS) Project Plan.* https://www.ngs.noaa.gov/GRAV-D/pubs/GRAV-D_V2007_12_19.pdf

Spector, A. and Grant, F.S. (1970). Statistical models for interpreting aeromagnetic data. *Geophysics.* 35(2): 293-302.

Strykowski, G. (2017). Airborne gravimetry and geoid mapping. A review of how airborne gravity is used in geoid studies.

Sylvester, O.E., Olujimi, F.O., and Sunday, A.O. (2018). On the determination of NTM and UTM positions from post processing of static DGPS observations on the Nigeria Minna Datum. *International Journal of Engineering Research Advancement Technology (IJERAT)*. 4(1):10-24. https://doi.org/10.31695/IJERAT.2018.3332

Sultan, S.A., Becker, R., Sturchio, N., Nasr, B., Milewski, A., El Alfy, Z., and Soliman, F. (2009). Mapping of subsurface structures in arid regions through integrated gravity, Magnetic, and seismic surveys: A case study from the Western Desert. Egypt. *Journal of Geophysical Research: Solid Earth*, 114(10): 241.

Tanko, A.I., Badamasi, M.M., Momade, S.B., and Yusuf, H.E.., Danjuma, M.M., and Sanusi, M.M. (2021). Access rights over land and water resources and implications on sustainable agriculture. In: the Niger-Benue Basins, a Report of Field Based Research funded under the National Research Fund (NRF) (2019-2021), Nigeria. *Tertiary Education Trust Fund (TEFFund)*. 45-53.

EDITOR-IN-CHIEF
Prof. W. F. HILL [MALAWI]

Tawey Mam, D, Alhassan, D.U, Adetona, A.A, Salako, K.A, Rafiu, A.A, and Udensi, E.E. (2020). Applications of aeromagnetic data to assess the structures and solid mineral potentials in part of North Central Nigeria. *Journal of Geography, Environment and Earth Science International.* 24(5): 11-29.

Telford, W.M, Geldart, L.P, and Sheriff, R.E. (1990). Classic text detailing Bouguer anomaly corrections and interpretation. Applied Geophysics 2nd ed. *Cambridge University Press.*

Telford, W.M, Geldart, L.P, and Sheriff, R.E, and Key, D.A. (1976). Applied Geophysics, Cambridge, London, Sydney: *Cambridge University Press.*

Thompson, D.T. (1982): A new technique for making computer-assisted depth estimates from magnetic data. *Geophysics,* 47(1): 31-37.

Tijani, M.N. (2008). Hydrochemical and stable isotopes, a comparison of saline gradients in the Benue basin, Nigeria. In: Adelana, S., MacDonald, A. Applied Groundwater Studies in Africa. *International Association of Hydrogeologists (IAH).* London, England. 13(1): 352-369.

Turner, D.C. (1983). Upper Proterozoic schist belts in the Nigerian sector of the Pan-African province of West Africa. *Precambrian research*. 21(1-2): 55-79.

Udensi, E.E, and Osazuwa, I.B. (2004). Spectral determination of depth to buried magnetic rocks under the Nupe Basin, Nigeria. *Nigeria Association of Petroleum Explorationists Bulletin.* (1): 22-27.

Uma, K.O. (1998). The brine fields of the Benue Basin, Nigeria: A comparative study of geomorphic, tectonic and hydrochemical properties. *Journal of African Earth Sciences.* 26(2): 261-275.

Uma, K.O. (1993). Nitrates in shallow (regolith) aquifers around Sokoto town. *Environmental Geology.* 21(1): 70-76.

UNEP (2010). United Nations Environment Programme. Lead pollution and poisoning crisis: Environmental Emergency Response Mission to Zamfara State, Nigeria. *United Nations Environmental Project (UNEP) Report.* Geneva Switzerland. https://www.unep.org/resources/assessment/lead-pollution-and-poiasoning-crisis-environmntal-emergency-response-mission-zamfara

UNICEF (1999). United Nations Children's Education Fund. A future global agenda for children: the links with Sanitation, Hygiene, Water and Environment. In: UNICEF Publication on Water, Sanitation and Hygiene (WASH). *Water Front Issue*. New-York, United States. 13(1): 12-15.

Usman, A.A., Wali, S.U., and Shera, I.M. (2024). Analysis of urban groundwater quality in dryland areas of Kebbi State. *The Journal of Experimental Life Sciences, Brawijaya University.* 14(3): 121-132. http://dx.doi.org/10.21776/ub.jels.2024.01403.04

Verduzco, B, Fairhead J.D, and Green C.M. (2004). New insights into Magnetic Derivatives for Structural Mapping. *The leading edge*. 23(2): 116-119. https://doi.org/10.119011.165

Waliu, S.U., Umar, K.J., and Abubakar, S.D. (2019). Hydro-geochemical characterization of shallow and deep groundwater in basement complex areas of Southern Kebbi State, Sokoto Basin, Nigeria. *Applied Water Sciences*. 9(1): 169-182 https://doi.org/10.1007/s13201-019-1042-5

Walracuens, K., Bakundukia, C., Mtoni, Y.E., and Camp, M.V. (2018). Understanding the hydrochemical evolution of groundwater in the Precambrian basement aquifers: A case study of Bugesera region in Burudi. *Journal of Geochemical Exploration*. 188(1): 24-42.

WGS (1984). Department of Defense World Geodetic System, 1984: Its definition and relationships with Local Geodetic Systems, Volume 8350 of DMA Technical Report Series of WGS 84 manual. *Defense Mapping Agency (DMA) now National Geospatial Intelligence Agency (NGIA)*

WHO (2011). World Health Organization Guidelines for drinking water quality. 4th Edition. Geneva, Switzerland. 7-15.

Wilcox, L.E. (1989). Gravity Data, advanced processing and gravity anomaly interpretation. In: James, D. *Encyclopaedia of Solid Earth Geophysics*. Dordrecht: Springer. 601-619.

Wright, J.B., Hastings, D., Jones, W.B., and Williams, H.R. (1985). Geology and Mineral resources of West Africa. *George Allen and Unwin*: London, 187.

EDITOR-IN-CHIEF
Prof. W. F. HILL [MALAWI]

Yilmaz, M., Yilmaz, I., and Uysal, M. (2018). Evaluation of Gravity anomalies based on global models by land gravity data. In: International Scholarly Scientific Research and Innovation. *World Academy of Science, Engineering and Technology, International Journal of Geological and Environmental Engineering.* 12(11): 814-820. Publications.waset.org/10009763pdf

Zhang, J., Peng, J., Chen, X., Shi, X., Feng, Z., Meng, Y., Chen, W., and Liu, Y. (2024). Comparative study on different interpolation methods and source analysis of soil toxic element pollution in Cangxi County, Meng, Guangyaaan City, China. *Sustainability.* 16(9): 3545-3561. https://doi.org/10.3390/su16093545

EDITOR-IN-CHIEF
Prof. W. F. HILL [MALAWI]